Reduced Fan Noise Radiation from a Supersonic Inlet

by

Kevin P. Detwiler

Thesis submitted to the Faculty of the
Virginia Polytechnic Institute and State University
in partial fulfillment of the requirements for the degree of

Master of Science

in

Mechanical Engineering

APPROVED:

Dr. Wing F. Ng, Chairman

Dr. R. A. Burdisso

Dr. R. G. Leonard

April 1993

Blacksburg, Virginia

REDUCED FAN NOISE RADIATION FROM A SUPERSONIC INLET

by

Kevin P. Detwiler

Dr. W. F. Ng, Chairman

Mechanical Engineering

(ABSTRACT)

A series of experiments was conducted to evaluate the aerodynamic and acoustic performance of a supersonic inlet with a modified auxiliary door geometry. A 1/14 scale model of an axisymmetric, mixed-compression, supersonic inlet designed for civil transportation was used in conjunction with a 10.4cm (4.1 in.) turbofan engine simulator to test a new inlet door geometry designed to reduce flow distortion and noise radiation. The new door geometry uses door passages with increased circumferential span to improve the distribution of the flow entering through the doors. In addition, the new design employs sonic flow velocity at the inlet throat and a converging flow passage in the auxiliary doors to attenuate propagating fan noise through the choking effect. To provide a basis for comparison, a baseline door geometry representative of current designs was also tested. The experiments were conducted at simulated aircraft takeoff engine speeds under static conditions. Steady-state measurements of the inlet flow field were made along with far field acoustic measurements of the fan noise. The results show the new door geometry is successful in reducing circumferential flow distortion at the fan entrance by a factor of 2.3 compared to the baseline configuration. In addition, far field radiation of the blade passing frequency tone and overall noise is reduced by an average of 4dB(SPL) in the forward and aft sectors (0° to 110° from the inlet axis). As a compromise for the distortion and acoustic improvements, the overall inlet total pressure recovery is reduced by approximately 2% with the new auxiliary doors.

Acknowledgments

I would like to take this opportunity to thank the many individuals who have contributed to this thesis and made my graduate studies a very memorable time. My sincere thanks to professors Dr. Robert G. Leonard, Dr. Ricardo A. Burdisso, and Dr. Wing F. Ng for giving their valuable time and insight while serving on my advisory committee. I am particularly grateful to Dr. Burdisso for his generous guidance in all matters acoustical. Furthermore, I sincerely thank Dr. Wing Ng for providing me with this opportunity, and enriching it with his encouragement and patience.

I would also like to thank Todd Ninneman, D. J. Osborne, Zhenguo Yuan, Abhijit Pande, and Terry Reid. I truly value their friendship and company - they have made my tasks more enjoyable, and I wish all of them the best of luck in all their endeavors. A special thanks to Zhenguo Yuan for taking the time to listen to a thousand crazy ideas about this research without laughing once, this thesis better because of it.

I also wish to thank my parents, Richard and Sigrid, and my brother, Brian, for their continuos support and encouragement throughout my engineering studies. And, finally, the most special thanks of all to Jennifer L. Herbst for her companionship and contributions during this endeavor. She assisted with the tests, suffered through the editing, brightened my days, and made the whole thing worthwhile.

Table of Contents

List of Illustrations

List of Tables

Nomenclature

BPF	blade passing frequency
dB	decibel, sound pressure level, reference pressure 20 x 10^6 Pascals
Hz	hertz, frequency
FFT	fast Fourier Transform
M	Mach number
Rc	Radius of the cowl lip
rpm	revolutions per minute
x/Rc	normalized axial position

1.0 Introduction

Although steady advancements in military aviation have made the technology for high speed flight available, most patrons of commercial air transportation have enjoyed only subsonic flight. Currently, however, there is growing interest in the development of a supersonic cruise aircraft for commercial transportation as globalized markets create a demand for faster long-distance transportation. A supersonic aircraft will significantly reduce the time required for long distance flights, an increasingly attractive feature to businesses with divisions throughout the world. Through the High Speed Civil Transport research program, NASA is developing designs for a supersonic-cruise passenger aircraft and is investigating the feasibility of using such an aircraft for commercial transportation.

Environmental impact constraints are an increasingly important consideration in the design of commercial transports, and are particularly challenging for the development of SST (supersonic transport) type aircraft. For a supersonic transport to be successful, its environmental impact must be minimized. The environmental issues surrounding a supersonic transport involve upper atmosphere emissions, airport community noise, and

the sonic boom. These topics are currently being researched to determine how their impact on the environment can be reduced.

Considerable effort is being invested to ensure that a supersonic transport will be able to meet the restrictions on airport community noise levels. Evaluations of an aircraft's impact on airport community noise levels focus primarily on noise generated while the aircraft is undergoing landing approach and takeoff. Although jet noise is expected to be the predominant noise source for SST aircraft, previous analysis by Trefny et al.[1] indicate that "forward propagated fan noise is a significant component during take off and approach." Many of the properties of the forward propagated fan noise are determined by the design of the engine inlet, in the case of an SST aircraft, a supersonic inlet. Unlike conventional subsonic inlets, supersonic inlets require many complex, variable features to perform at both subsonic and supersonic flight speeds. The features typically include a translating centerbody, boundary-layer bleed systems, and auxiliary inlet doors which compensate for the small capture area of the inlet during subsonic flight. The effects of these features on the radiated engine noise are currently being investigated.

Under the Supersonic Cruise Aircraft Research program in 1983, NASA Lewis conducted a program to determine experimentally the low speed aerodynamic and acoustic performance of a representative supersonic inlet. A 1/3 scale model of an axisymmetric, mixed-compression supersonic inlet was coupled to a 0.4 scale JT8D refan simulator and tested in the NASA Lewis 9x15 foot anechoic wind tunnel. The tests were conducted at windtunnel airspeeds of Mach 0 to 0.2 to simulate low speed flight. The results of the

research are detailed in references 1 through 8. The acoustic research, references 7 and 8, concentrated on the far-field radiation of the fundamental blade-passing-frequency tone and the broadband noise. One of the principal findings was that opening the auxiliary inlet doors significantly increases the fundamental blade-passing-frequency tone. It was suspected that the increase in tone was caused by the auxiliary doors increasing the flow distortion at the fan entrance.

Recently, an experimental test program was initiated at Virginia Polytechnic Institute and State University to reduce the impact of a supersonic transport on airport community noise. The program, focusing on the radiation of turbomachinery noise from a supersonic inlet, involves the testing of a 1/14 scale supersonic inlet coupled to a 10.4 cm(4.1in) turbofan engine simulator. The small scale of the inlet and simulator was selected to provide a lower experiment cost, simplifying the investigation of design modifications. Due to the number of variable features associated with a supersonic inlet, the experimental test matrix can be large. The small-scale inlet and simulator provide initial results and trends before a design is considered for testing in a more costly, large-scale test program.

Under the VPI test program, Nuckolls and Ng[17] developed a modified auxiliary inlet door geometry designed to reduce the radiated fan noise from a supersonic inlet. The new auxiliary doors were designed to include two noise attenuating features: an increased circumferential span to provide more uniform air distribution to the engine, and a converging door passage area to employ the choking effect in the auxiliary doors. When

tested at simulated landing-approach conditions and compared with results from the original-geometry doors, the modified doors reduced flow distortion by a factor of two and lowered forward radiated fan noise by 6dB. The objective to reduce noise by modifying the auxiliary door is believed to be unique to the VPI test program because there is no known previous research with this goal.

The current research focuses on evaluating the acoustic and aerodynamic performance of the modified auxiliary door geometry at simulated aircraft takeoff conditions. During landing approach (the conditions simulated by Nuckolls and Ng[17]), the aircraft's engines are typically throttled back to a lower speed and the fan noise is dominated by the blade-passing-frequency tone. For aircraft takeoff, the engines are operated at design speed and the fan noise is comprised of a series of distinct tones called combination tones. The objective is to determine how the modified auxiliary doors perform with the higher level of inlet airflow and combination tone fan noise representative of aircraft takeoff conditions.

The supersonic test inlets and basic test procedures developed by Nuckolls and Ng[17] are used in the current research. The acoustic results are extended to include the radiation of overall noise in addition to the blade-passing-frequency tone; overall noise is useful because it includes the contributions of the combination tones generated at the higher fan speeds.

This thesis is organized into four chapters. The next chapter outlines the experimental setup and procedures for the test program, the detailed modifications to the

auxiliary door geometry, and the physical dimensions and acoustic properties of the turbofan engine simulator. Chapter 3 presents the aerodynamic and acoustic results of the test program. A summary of the conclusions and a discussion of potential areas of future research are presented in Chapter 4. Finally, the results from tests with the auxiliary doors closed and an experiment involving an acoustic baffle are presented in Appendices A and B respectively.

2.0 The Experiment

This chapter describes the setup of the experiment. Section one outlines the specifications and acoustic properties of the turbofan simulator. The second section describes the supersonic test inlets and auxiliary inlet door geometries. The instrumentation and procedures for the aerodynamic and acoustic tests are discussed in the final two sections.

2.1 Turbofan Simulator

The supersonic inlets were tested in conjunction with a Tech Development, Model 460 turbofan engine simulator which was used to drive the inlet airflow and to provide the characteristic engine noise signal. The Model 460, used in previous aerodynamic test programs to simulate a Pratt and Whitney JT9D turbofan engine, is similar to the model used by Pratt and Whitney to perform acoustic research [11,12]. Figure 1 shows the turbofan simulator and its rotating components. The Model 460 has a single-stage fan section consisting of 18 fan blades (tip radius 2.05 in.) and 26 stators. A single-stage turbine, driven by compressed air, supplies power for the fan. The simulator, instrumented with a magnetic-pickup tachometer and bearing thermocouples, has a design speed of 80,000 RPM.

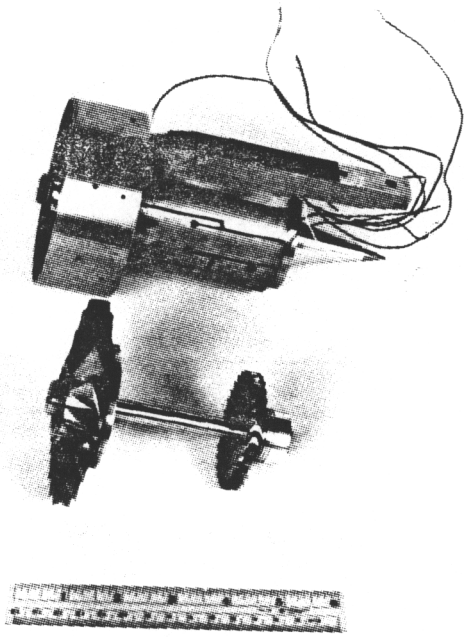

Figure 1. Turbofan Engine Simulator

The simulator was considered appropriate for this acoustic investigation because it generates a fan noise signal representative of full-size aircraft engines. During takeoff, the engines under consideration for use in an SST aircraft are expected to generate noise with a "combination tone" spectrum. A review of the noise characteristics of aircraft engines, including an explanation of combination tones, is given by Cumpsty [16]. The noise from a high-speed fan is typically divided into two types: pure tone and combination tone (or multiple pure tone). Examples of these noise spectra are shown in Figure 2. Pure tone fan noise is characterized by a prominent tone at a frequency equal to **BN**, where **B** is the number of fan blades and **N** is the rotational speed of the fan. This frequency, referred to as the Blade Passing Frequency or BPF tone, is created by the interaction of the fan blade wakes with the stator row and by the passage of distorted flow into the fan. Combination tone fan noise is characterized by a series of tones located at integer multiples of the fan rotational speed (or $\mathbf{f_k = kN}$, $\mathbf{k} = 1,2,3 \ldots$). The tones are created when the fan tip velocity becomes supersonic relative to the flow entering the fan. The fan blades shed shock waves in the upstream direction that vary in strength due to small differences in the blade profiles. The shock waves coaless and cancel as they propagate the length of the inlet to form the combination tone frequency spectrum illustrated in Figure 2. Combination tones typically occur in addition to the BPF tone generated by the subsonic portion of the fan.

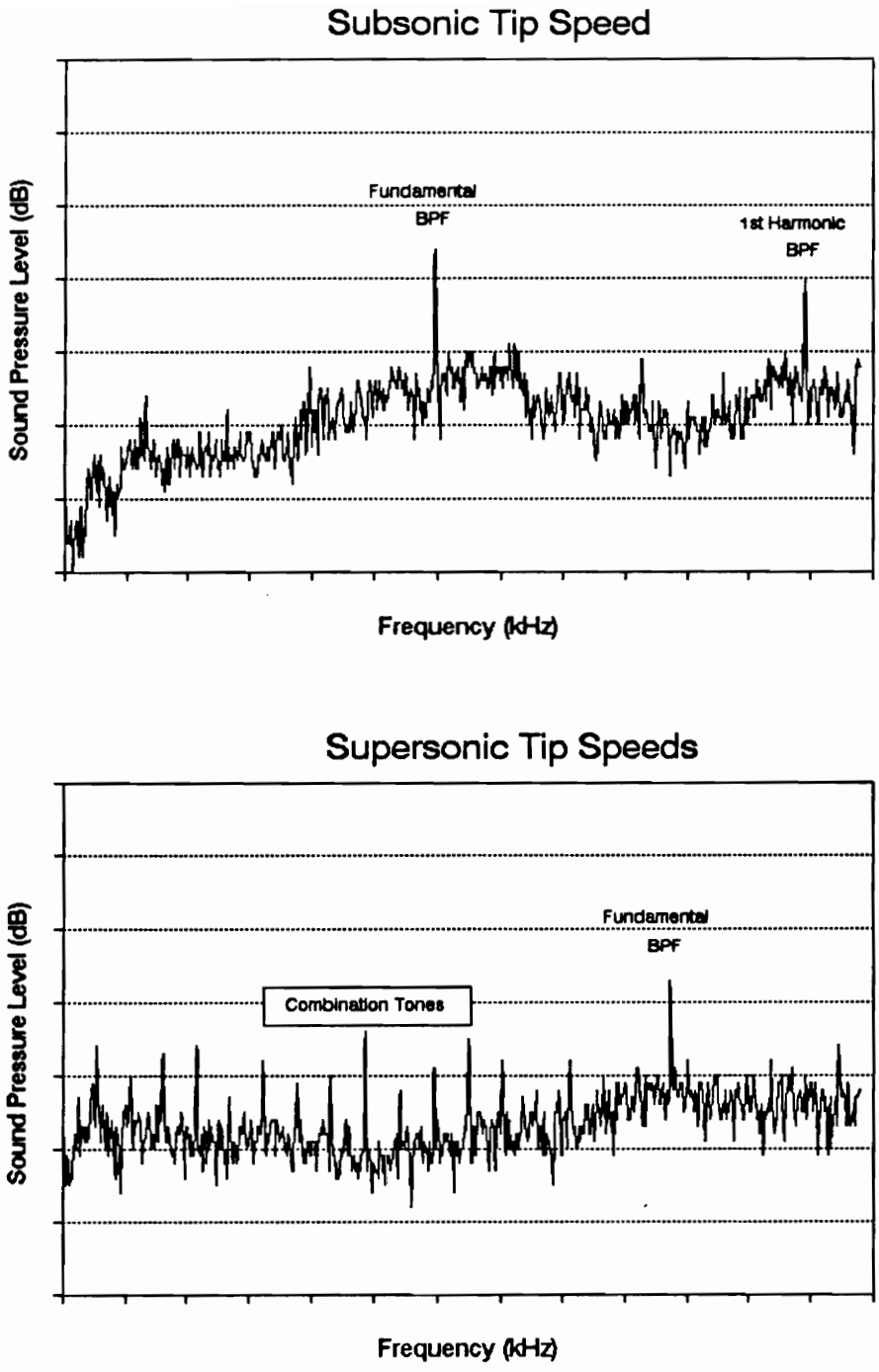

Figure 2. Typical Fan Noise Spectra, Subsonic and Supersonic Fan Tip Speeds

The Model 460 simulator attains supersonic fan tip velocity at a rotational speed of approximately 65,000 RPM, or 80 PNC (percent corrected design speed). At rotational speeds of 80 PNC and above, the simulator generates fan noise with a combination tone spectrum. For the simulated aircraft takeoff tests conducted in this experiment, the simulator was operated at 88 PNC. This engine speed was selected due to limitations on the compressed-air supply (used to power the simulator) at the test facility. Although the simulator was not operated at design speed, the test speed (88 PNC) did provide the combination tone spectra representative of full-size engines during aircraft takeoff.

Another important acoustic characteristic of the simulator, the propagation behavior of the rotor-stator interaction noise in the inlet passage, is determined by the relative number of fan blades to stator blades. Tyler and Sofrin[18] developed a theory, based on interaction kinematics and a superposition of rotating pressure modes, which predicts that all modes of the rotor-stator interaction noise will decay rapidly in the inlet passage if the number of stators is at least twice the number of rotors; in this condition, the rotor-stator noise is commonly refered to as being "cut-off". In the case of the Model 460 simulator, the number of stators is less than twice the number of rotors (18 blades, 26 stators), so that some noise modes from the rotor-stator interaction are expected to propagate in the inlet. Thus, the simulator is classified as having a "cut-on" rotor-stator interaction noise.

2.2 Supersonic Test Inlet

The test inlet used in this experiment is based on the axisymmetric, mixed compression "P-inlet" model developed by NASA. In 1983 the inlet model was used by researchers at NASA Lewis to determine the aerodynamic and acoustic performance of a representative supersonic cruise inlet. A cutaway drawing showing the configuration of the NASA P-inlet is shown in Figure 3. Designed for an aircraft cruise speed of Mach 2.65, the NASA P-inlet incorporates several variable features, including: a translating centerbody, boundary layer bleed systems, and auxiliary inlet doors. The translating centerbody is designed to permit control of the inlet throat area to maintain the desired shock structure inside the inlet at supersonic cruise speeds. The cowl and centerbody bleed systems are used to prevent boundary layer buildup on the inlet walls. The boundary layer is minimized to avoid shock-boundary layer interaction problems at aircraft cruise speeds. The auxiliary inlet doors are required to provide sufficient mass flow to the engine at low flight speed conditions. During aircraft takeoff and approach, the capture area of the P-inlet is too small to meet the airflow requirements of the engine; therefore, the auxiliary doors are opened to increase the capture area of the inlet.

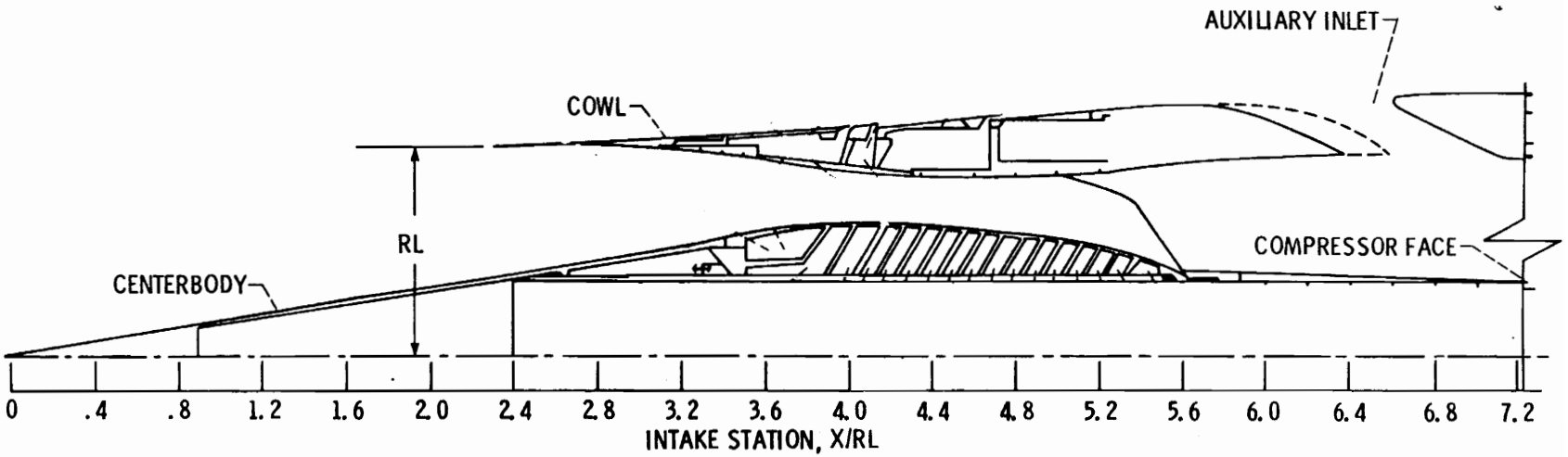

Figure 3. Schematic of NASA P-Inlet (ref. 8)

A cutaway sketch of the supersonic test inlet used in the current experiment is shown in Figure 4. The test inlet, essentially a 1/5 scale model of the NASA P-inlet, incorporates the aforementioned variable features of the NASA P-inlet except for the cowl and centerbody bleed systems. The aerodynamic results of [8] show the bleed systems to provide negligible boundary layer reduction at low flight speeds. In addition, the concerns of shock-boundary layer interaction do not apply to subsonic flight (aircraft takeoff and approach). For these reasons, the cowl and centerbody bleed systems were not incorporated into the design of the current test inlet.

The translating centerbody assembly is supported by four equally spaced struts located near the entrance of the fan. For this experiment, the centerbody was kept in the fully retracted (take off and subsonic cruise) position. The cross-section of each strut, also shown in Figure 4, was designed to minimize the strut wake shed into the fan. Although the wakes shed by the struts are recognized as a source of fan noise generation, the centerbody support struts are an integral part of the mechanical design of the P-inlet and therefore have been included in the test inlet.

2.3 Auxiliary Door Configurations

The two auxiliary inlet door geometries evaluated in this experiment are shown in Figure 5. The auxiliary doors shown in Figure 5a feature the same geometry as the fully-open auxiliary doors of the NASA P-inlet. This configuration, representing the current P-inlet design, will be referred to as the Baseline inlet. The Baseline inlet has four evenly

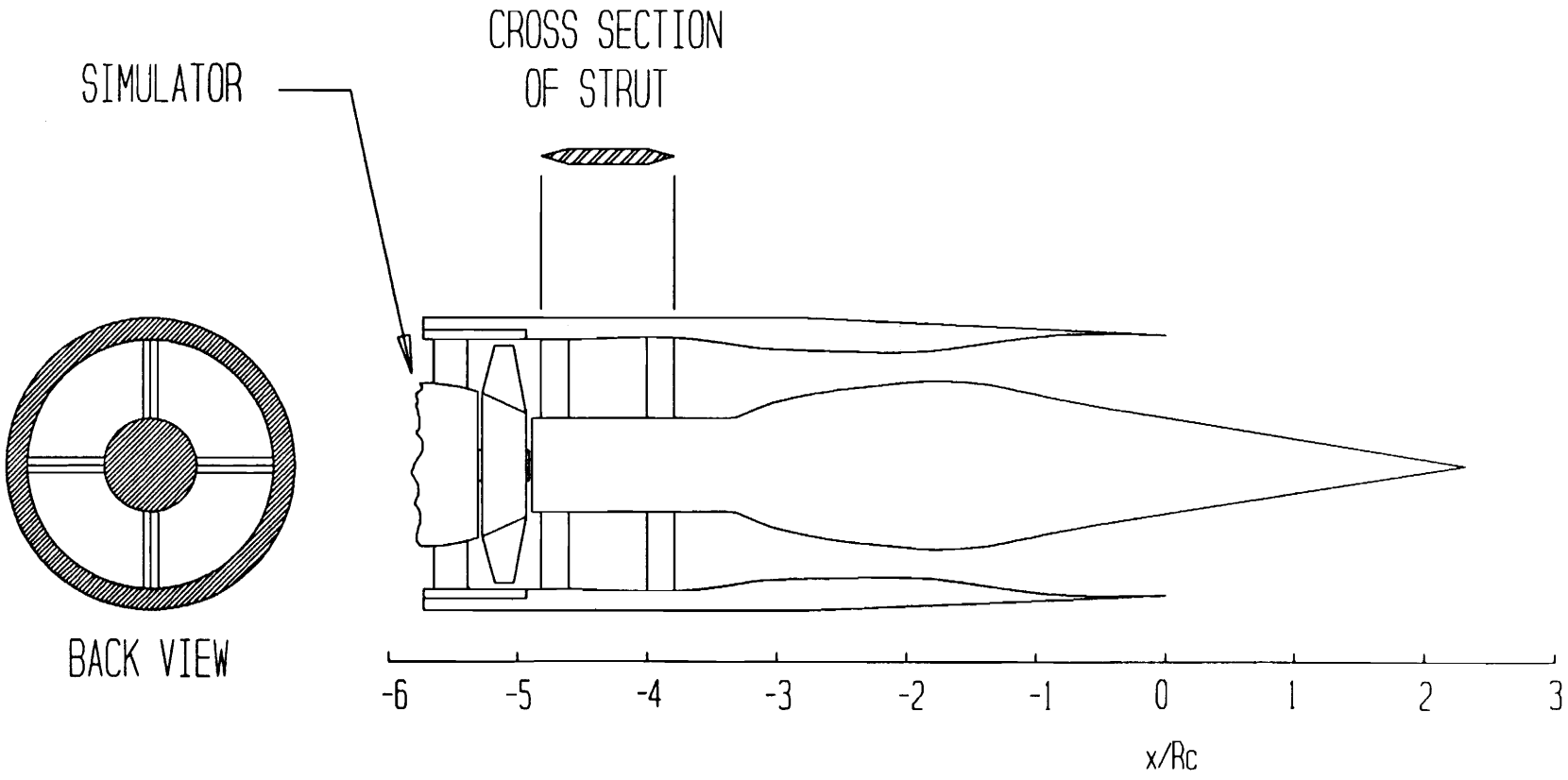

Figure 4. Schematic of Supersonic Test Inlet

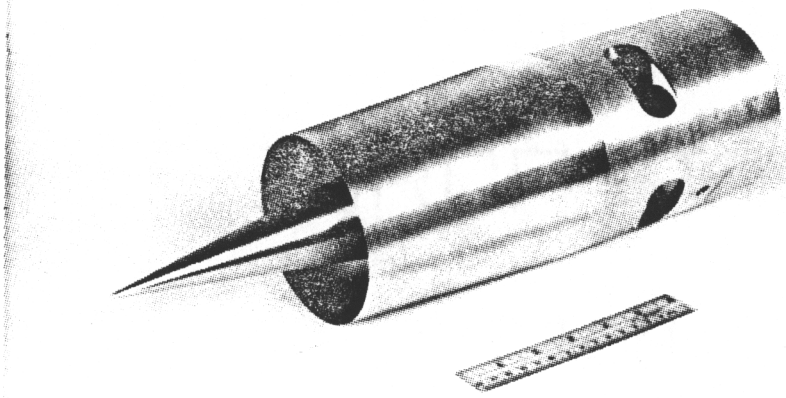

5a. Baseline Inlet

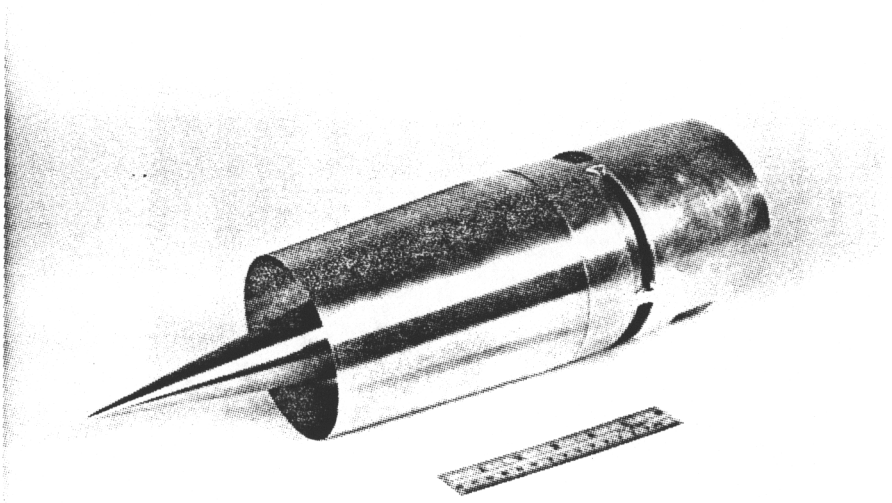

5b. Modified Inlet

Figure 5. Baseline and Modified Inlets

spaced auxiliary inlet doors, each spanning 50°. The combined capture area of the four Baseline doors is 9.8 in^2 (63.2cm^2) and the combined cross-sectional area of the door passages is 5.7 in^2 (36.8cm^2).

The inlet shown in Figure 5b features a modified door geometry designed to reduce inlet flow distortion and radiated fan noise. This inlet configuration will be referred to as the Modified inlet. Figure 6 illustrates the differences in geometry between the Baseline and Modified doors. The Modified doors are designed with increased circumferential span (83° versus 50°) to improve the distribution of the flow from the auxiliary doors and, consequently, to reduce flow distortion at the fan entrance. The doors of the Modified inlet also feature a converging flow path intended to reduce fan noise propagation through the auxiliary doors by inducing high flow velocity in the doors. A high Mach number in the door passage will increase the time required for a noise signal to propagate through the door, thereby dissipating more of the signal energy. This process of noise attenuation, referred to as the "choking effect", is expected to occur for Mach numbers greater than 0.5 (ref. 8). Although the Modified inlet doors have a combined capture area equivalent to that of the Baseline doors, the converging flow path design reduces the combined throat area of the doors to 2.6in^2 (16.6cm^2), a 55% reduction from the Baseline configuration.

In addition to the Baseline and Modified door configurations, the inlet was evaluated with the auxiliary doors closed. This inlet configuration was accomplished by

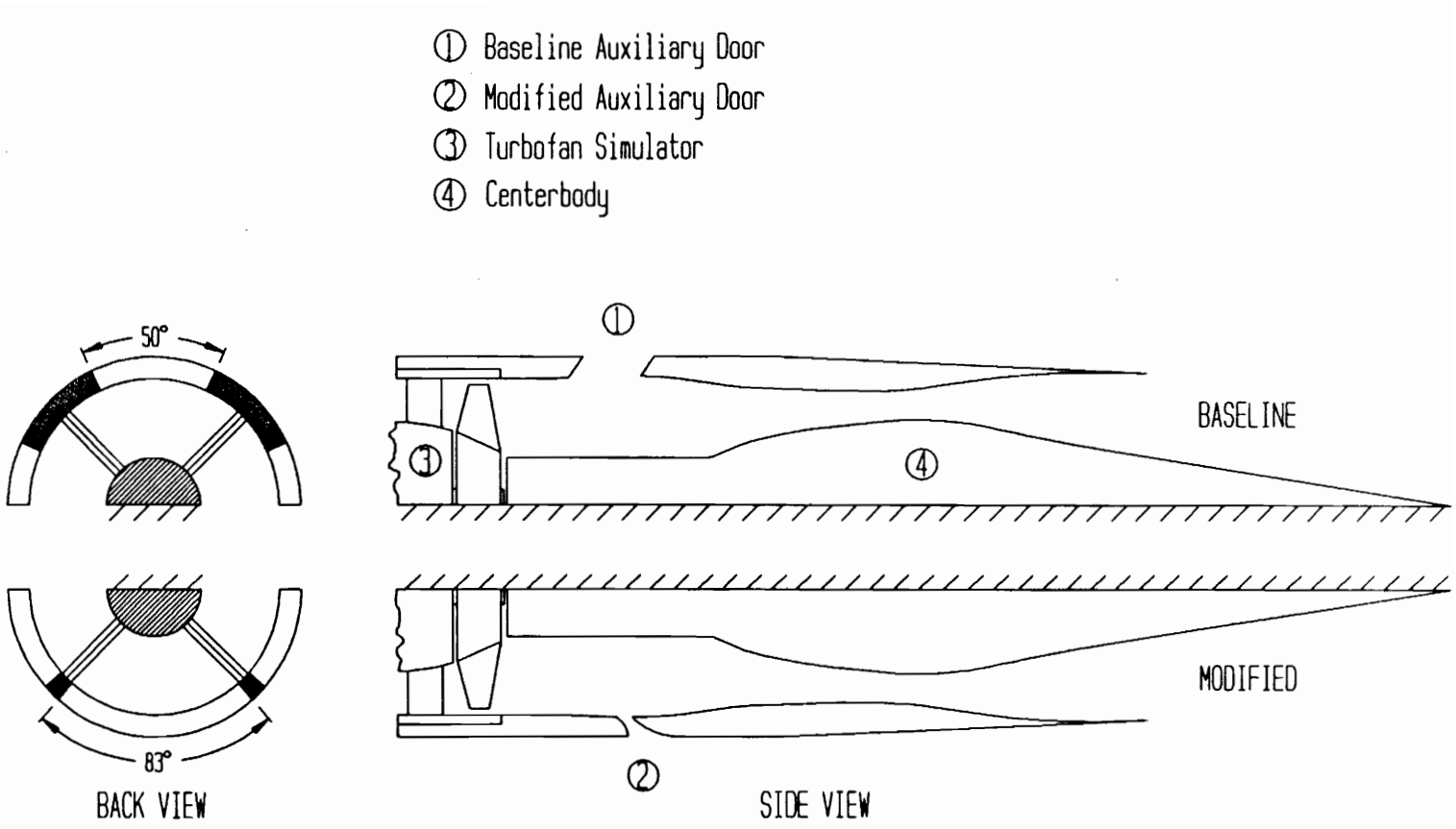

Figure 6. Auxiliary Door Geometries (Baseline vs. Modified)

covering the Modified doors with a 0.25 inch (0.64 cm) thick aluminum band to prevent airflow through the door passage and to minimize acoustic transmission. The acoustic and aerodynamic results from the closed door evaluation are presented in Appendix B.

2.4 Test Set-up

The aerodynamic and acoustic tests for this experiment were conducted at an outdoor facility. The test facility equipment consisted primarily of an air compressor and a high-pressure air line that supplied compressed air to the simulator turbine. The speed of the simulator was controlled with a valve that throttled the supply of compressed air. All acoustic measurements were made with the engine simulator and microphones mounted 48in (122cm) above a level surface of mowed lawn.

Evaluating the acoustic performance of an aircraft engine at an outdoor facility requires special consideration of inlet flow distortions created when static, ambient air is drawn into the inlet. Figure 7 demonstrates two mechanisms that can generate significant inlet flow distortions during a stationary engine test. First, mild atmospheric turbulence can be lengthened and intensified as it is drawn into the inlet, as shown in the lower diagram. This elongated and intensified turbulence creates unsteady blade loading and increased fan noise levels. Secondly, it is possible for the engine to generate a vortex from the boundary layer created as the ambient air flows past the ground beneath the engine. This phenomenon, called a "ground vortex," can create an intense region of vorticity at the fan entrance, and increase the noise generation of the fan.

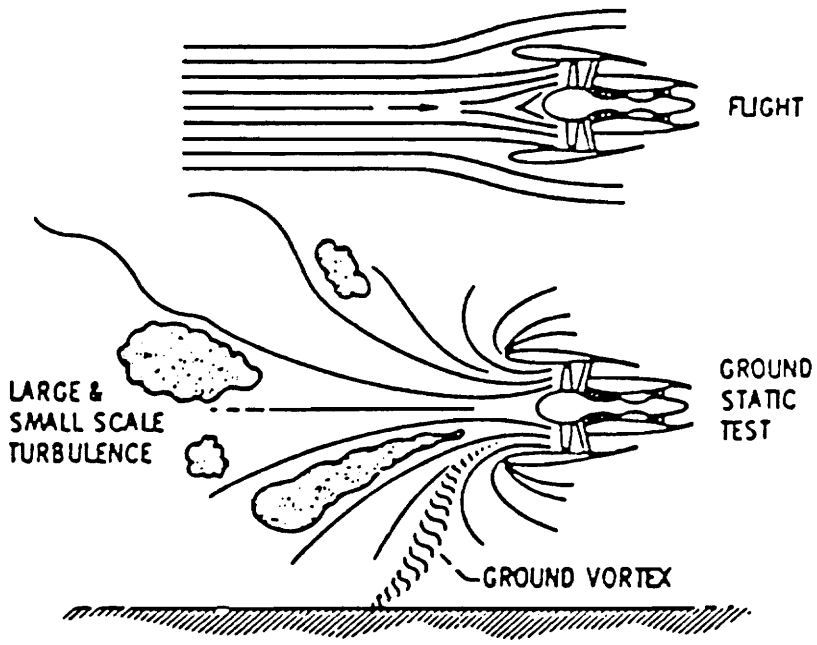

Figure 7. Mechanisms for Flow Distortion During Static Testing (ref. 15)

In general, the testing of aircraft engines under static conditions is expected to increase the level and variability of the fan generated noise. To compensate for noise variations due to random atmospheric turbulence, multiple acoustic readings were averaged for each microphone position and inlet configuration (the averaging methods used are discussed in section 2.6.1). The possibility of inducing a ground vortex was reduced by placing the simulator 48 in (122 cm) above the ground.

2.5 Aerodynamic Measurements

Measurements of total pressure recovery and flow distortion were used to compare the overall aerodynamic performance of the Baseline and Modified inlets. Aerodynamic measurements also contributed to the interpretation of the acoustic results. The acoustic performance of an aircraft engine is closely tied to the aerodynamic behavior of the inlet. One objective of the current research program is to better understand the influence of aerodynamics on the acoustic performance of the inlets.

Total pressure and Mach number measurements were made at the four probe stations shown in Figure 8. These locations will be referred to as the cowl lip, throat, fan face, and fan exit stations. In a previous experiment conducted by Nuckolls[17], the flow upstream of the auxiliary doors was shown to be axisymmetric. Therefore, measurements for the cowl lip and throat stations were taken at only one circumferential angle. The throat Mach number data was taken at the center of the throat passage (x/Rc = 1.93, r/Rc

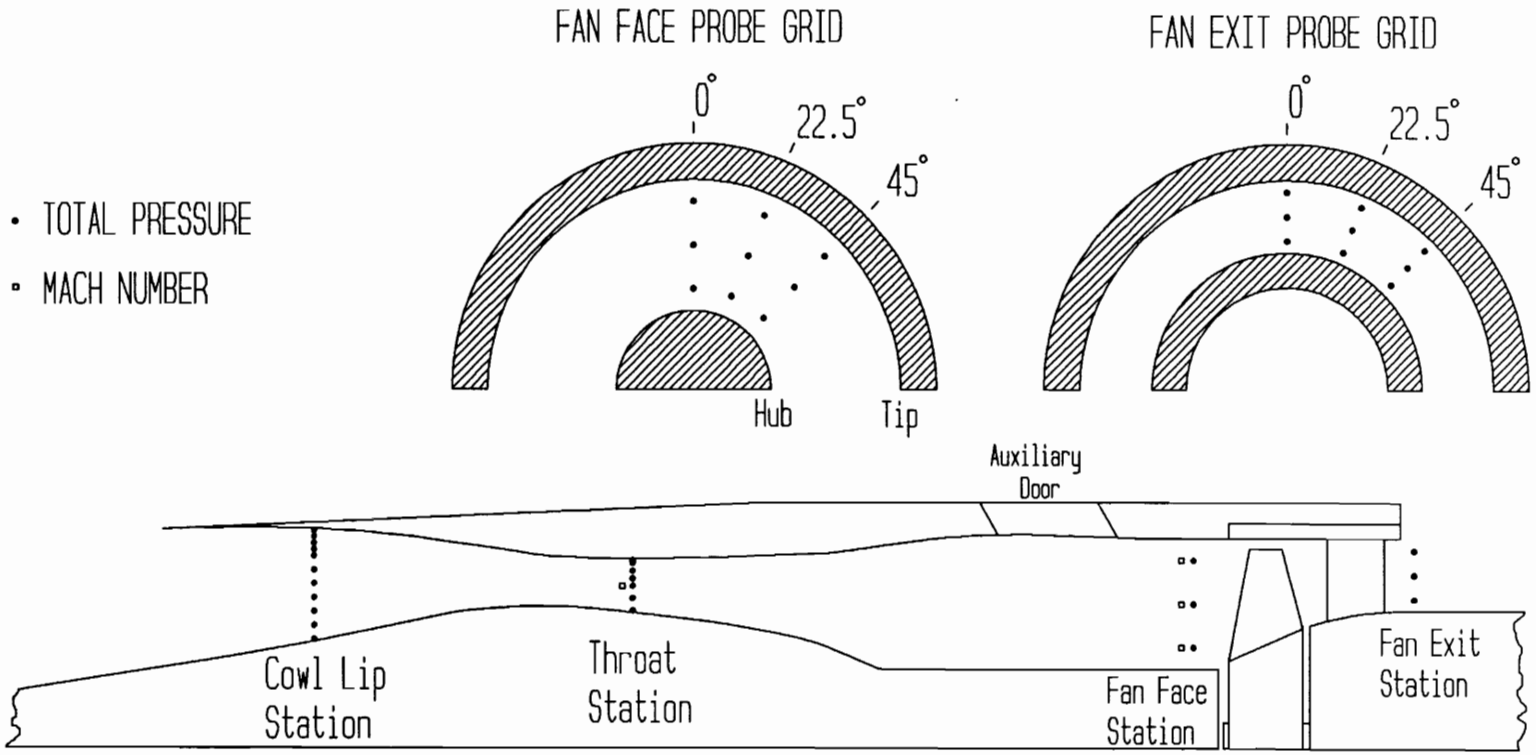

Figure 8. Aerodynamic Instrumentation of Supersonic Test Inlet and Simulator

= 0.74). Multiple-point probe traverses, shown in Figure 8, measured the total pressure at the cowl lip and throat locations.

The flow field in the region of the fan face is non-axisymmetric due to the influence of the flow from the auxiliary doors. The Mach number and total pressure distributions at the fan face station were resolved with the nine-point probe grid shown in Figure 8. The measurement grid spans from the center of the support strut (0°) to the center of the auxiliary door (45°). For the measurements at 0°, it was necessary to remove the support strut at that location (However, the acoustic measurements were taken with all four struts in place). A similar probe location grid, also shown in Figure 8, was used to measure the total pressure distribution at the fan exit.

The aerodynamic measurements were made with two conventional pressure probes. A 1/16 in (1.6 mm) diameter pitot-static probe was used for static and total pressure measurements at the throat and fan face stations; the Mach number was then calculated isentropically from the measured static and total pressures. To measure the total pressure at the cowl lip and fan exit stations, a 1/16 in (1.6 mm) diameter Kiel probe was selected for its higher tolerance of flow angularity.

2.6 Acoustic Measurements

2.6.1 Instrumentation

Two Bruel and Kjaer model 4136 condenser microphones were used to measure the acoustic field. The microphones have a 0.25in (0.64cm) diameter diaphragm, and provide linear responses for frequencies up to 30kHz. The microphones were used in conjunction with a Bruel and Kjaer microphone power supply. Both microphones were calibrated prior to testing with a Bruel and Kjaer pistophone providing a 120dB signal at 5000Hz.

The microphone signals were analyzed on a Bruel and Kjaer model 2030, dual channel spectrum analyzer. The spectrum analyzer performed narrow-bandwidth FFT (fast-Fourier transform) conversions of the acoustic data. The upper frequency limit of the spectrum was set at 25.6kHz, providing a spectrum bandwidth of 32Hz. The FFT results from the spectrum analyzer were used to record the BPF tone level and to investigate other fan related tones. Sample noise spectra were transferred from the signal analyzer to a personal computer for permanent storage.

To compensate for the effects of random atmospheric turbulence, the analyzer was configured to calculate the linear average of ten consecutive noise spectra. In addition, ten consecutive values of average BPF tone level were recorded at each microphone position.

In addition to the Fourier analysis, the microphone signals were also measured on an RMS voltmeter. The RMS voltage was used to calculate the overall sound pressure level (OASPL) of the acoustic signal. The OASPL represents the integration of the noise spectrum over the frequency range. The range of the voltmeter reading during each acoustic measurement was recorded for uncertainty analysis.

2.6.2 Microphone Locations

The acoustic measurements were made in two test configurations. For the primary test configuration, shown as a plan view in Figure 9, the microphones were placed along a circular arc centered at the intersection of the inlet axis and the inlet entrance plane (x/Rc = 0). A radius of 48 inches (122 cm) was selected for the microphone location arc to provide measurements in the far-field (i.e., KL >> 1). The eleven microphone measurement points were located at ten degree increments (0° to 110°) from the inlet centerline axis. Microphone stands were used to place the microphones 50in (127cm) above the ground, level with the inlet centerline.

In the second test configuration, an acoustic baffle was used to further investigate the noise radiation properties of the inlets. The baffle was constructed to allow selective isolation and measurement of the different noise sources of the inlet (i.e., the inlet mouth, auxiliary doors, and fan exit). The configuration and results of the acoustic baffle test are presented in detail in Appendix B.

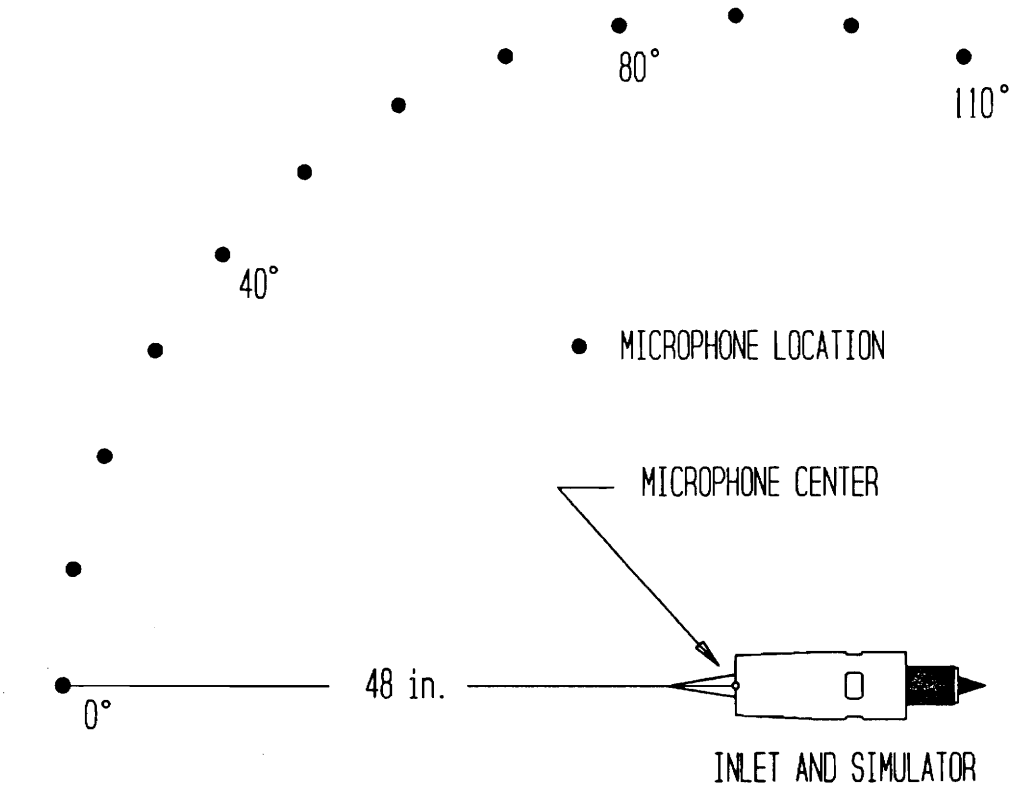

Figure 9. Microphone Layout, Plan View

3.0 Results and Discussion

The results are divided into aerodynamic and acoustic sections. The aerodynamic results demonstrate the reduced flow distortion of the Modified inlet and present the overall aerodynamic performance of the inlets. The acoustic results illustrate the characteristics of the radiated noise, and demonstrate the improved acoustic performance of the Modified inlet.

3.1 Aerodynamic Results

3.1.1 Inlet Distortion

Flow distortion is an important consideration in the design of aircraft inlets. Distorted flow will decrease the stall margin of an engine and increase the generation of fan noise. The Modified auxiliary doors are designed to reduce flow distortion in the supersonic inlet. This section compares the total pressure and Mach number distributions at the fan stations of the Baseline and Modified inlets to evaluate changes in flow distortion.

Before presenting the inlet distortion results, it is important to illustrate how flow distortion affects the acoustic performance of an aircraft engine. It is crucial to understand the difference between radial and circumferential gradients and their influence on noise generation. Figure 10 shows two hypothetical examples of velocity distortion at the entrance of an engine. The first diagram depicts velocity distortion with gradients in the radial direction only. In a flow distribution of this nature, any point along the span of a rotating fan blade will encounter air of constant axial velocity. For example, a point at mid-span will encounter only Mach 0.3 air. Thus, with distortion comprised of radial gradients, the blade loading remains constant as the fan rotates and noise generation is minimal. The second diagram in Figure 10 illustrates axial velocity gradients in the circumferential direction only. In this flow distribution, a rotating fan blade will encounter different axial velocities depending on its angular position. For example, any point on the fan blade will be exposed to a 30% reduction in axial Mach number between 35° and 45°. As each fan blade passes through the change in Mach number, the pressure in that region fluctuates. If the fan is rotating at a constant speed, the periodic pressure fluctuations are received as noise at multiples of the blade-passing frequency of the fan. Therefore, unlike radial gradients, circumferential gradients of flow distortion will increase the noise generation of an aircraft engine.

The measured total pressure distributions at the fan face stations of the Baseline and Modified inlets are presented as contour plots in Figure 11. The plots represent a 90° portion of the annular inlet passage at the entrance of the fan. The symmetry of the

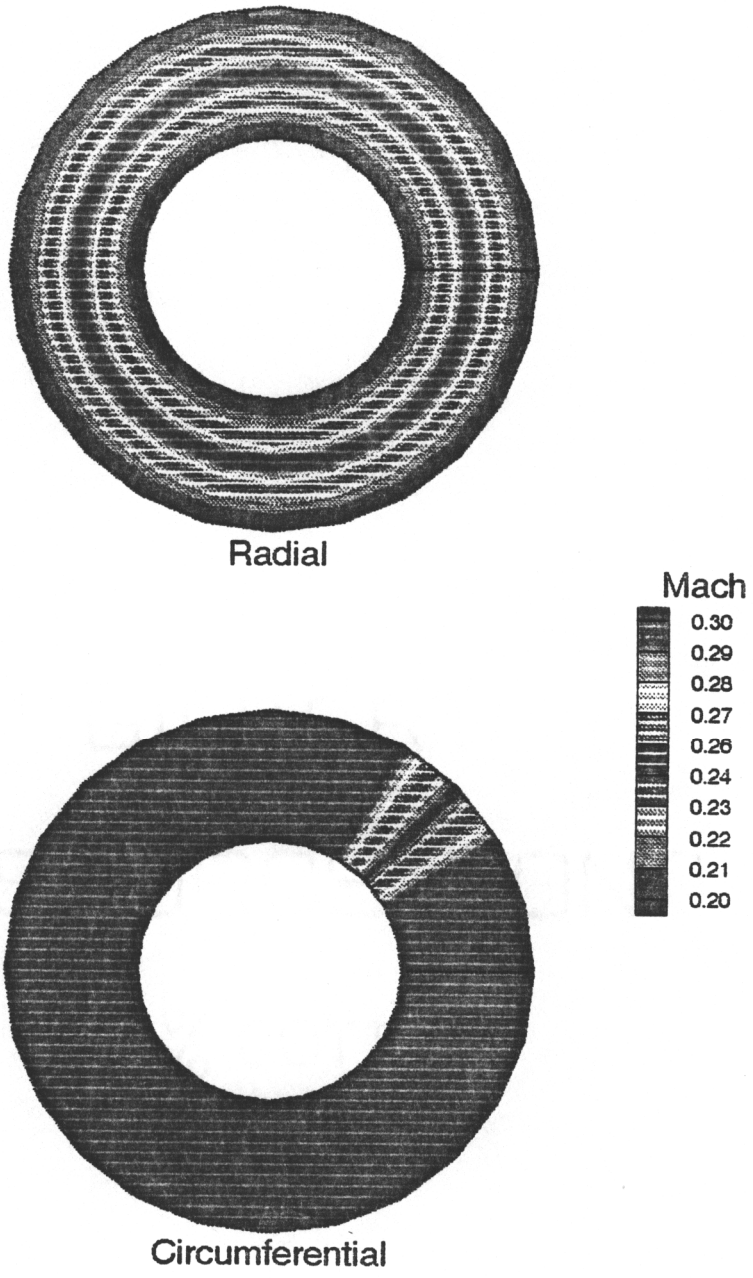

Figure 10. Hypothetical Gradients of Axial Velocity Distortion at the Fan Face

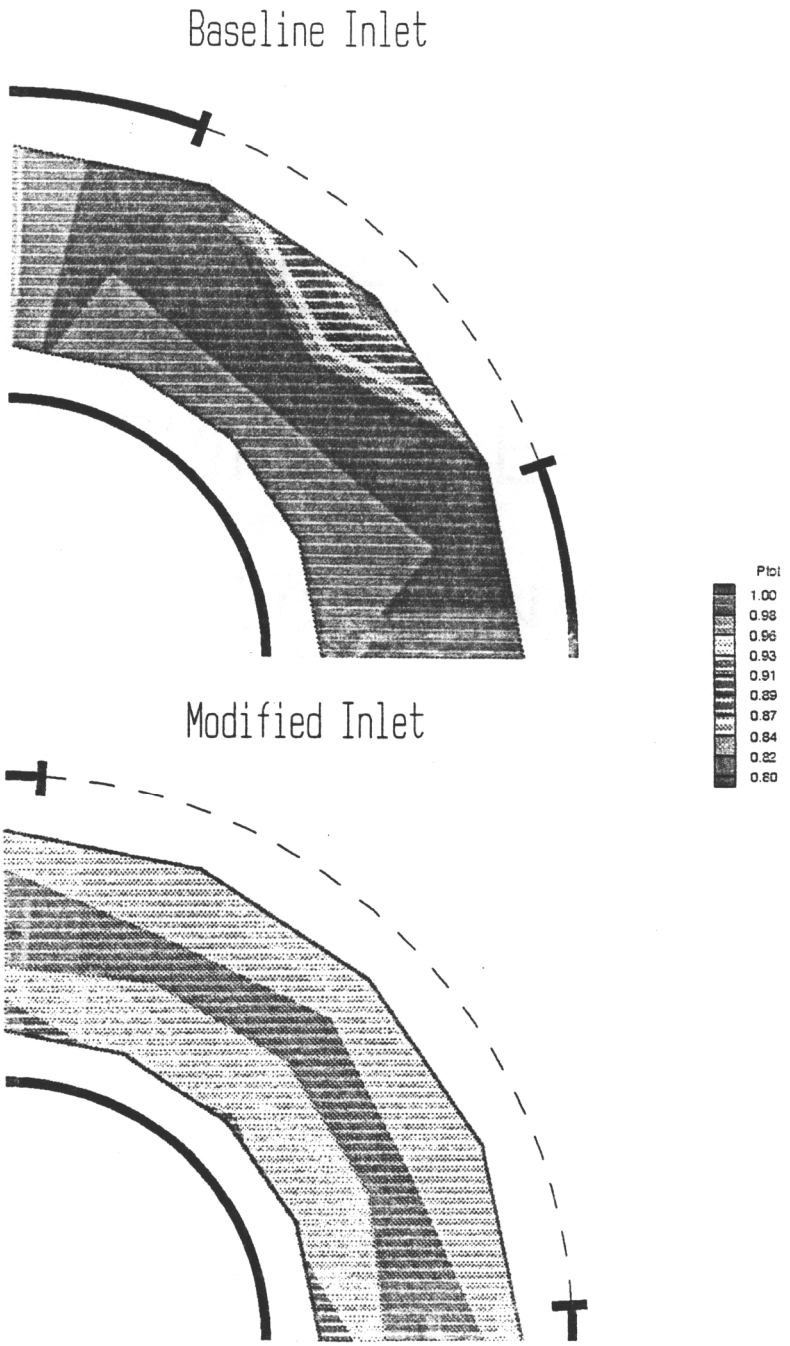

Figure 11. Total Pressure Distribution at the Fan Face, 88 PNC

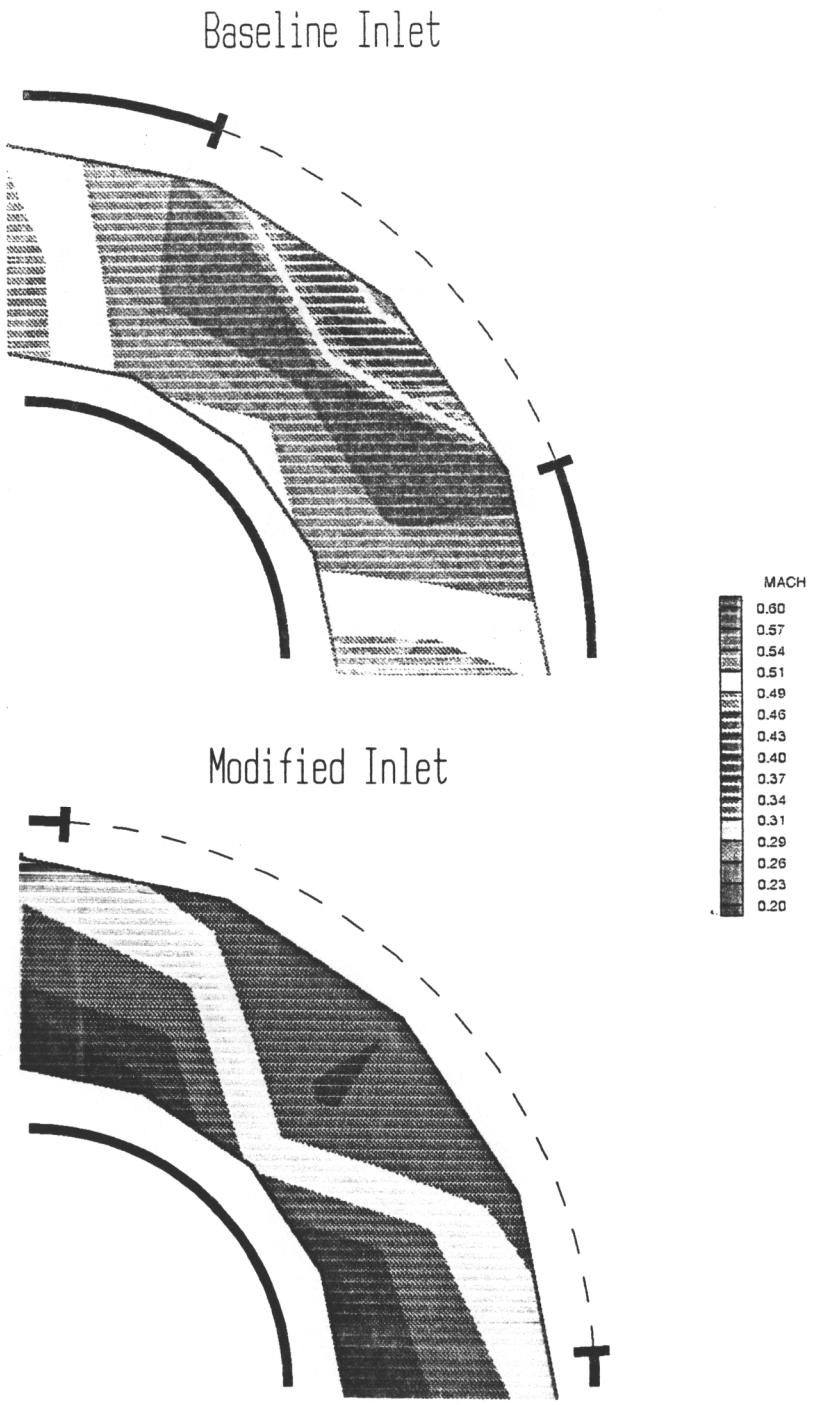

Figure 12. Mach Number Distribution at the Fan Face, 88 PNC

auxiliary door construction enabled the extension of the 45° probe grid to the 90° contour plots shown. The approximate locations of the inlet walls and auxiliary inlet doors are indicated on the plots. Because the contour lines are interpolated between the data point but are not extrapolated to the walls of the inlet, the contour plots do not include the narrow segments of area near the hub and tip walls of the inlet passage.

The contour for the Baseline inlet shows 98% to 99% total pressure recovery at all measurement points except near the tip wall, in the vicinity of the auxiliary door centerline. This low total pressure region is most likely caused by a separation of the flow entering through the auxiliary door. The region of separated flow creates a steep circumferential gradient of total pressure in the tip region of the fan. As discussed previously, flow distortions of this nature are expected to increase the generation of fan noise.

The total pressure distribution for the Modified inlet shows an increase of approximately 5% in total pressure losses near the hub and tip walls compared to the Baseline inlet results. The Modified inlet does not, however, show a concentrated region of high total pressure loss in the vicinity of the auxiliary door. This indicates that separation of the auxiliary door flow has been reduced with the Modified door geometry.

The axial Mach number distribution contours, shown in Figure 12, support the observations from the total pressure distribution plots. The axial Mach number contour for the Baseline inlet shows a region of low velocity near the tip wall, in the vicinity of the auxiliary door centerline. The low velocity in this region is, again, most likely the result of flow separation at the downstream edge of the Baseline auxiliary doors. The Mach

number in the region of the fan tip changes from 0.6 to 0.2 within an angular distance of 22.5°. An axial velocity gradient of this magnitude will cause significant fluctuations in the blade loading, resulting in increased fan noise generation.

The Mach number contour for the Modified inlet does not show a region of low axial velocity near the tip wall. In the tip region of the Modified inlet, the axial Mach number changes by only 0.05 throughout the 90° range of the contour plot. This indicates that the increased span of the Modified doors improves the distribution of the door flow, and significantly reduces separation at the downstream edge of the door. It is possible that a small degree of flow separation is present in the Modified inlet, beyond the outer radius of the probe location grid. However, this region of separation would still be considerably smaller than that measured in the Baseline inlet. Thus the data show that the first objective of the Modified door design, improved auxiliary door flow distribution, has been accomplished.

Quantified values of circumferential distortion are useful for comparing the performance of the two inlet configurations. Values of circumferential distortion, given by the formula **(Mmax - Mmin)/Mave**, were calculated for each of the three radial positions at the fan face station. These values were then averaged by area-weighting to yield the overall circumferential distortion values shown in Table 1. Compared to the Baseline configuration, the modified auxiliary doors reduce circumferential distortion of the axial Mach number by a factor of 2.3. Table 1 also shows the circumferential distortion results from Nuckolls[17] for the same inlets tested at a fan speed of 60PNC. The current

reduction in circumferential distortion is consistent with the results of the lower fan speed, although the reduction factor has increased slightly for the current test. Nuckolls[17] demonstrated that a reduction in circumferential distortion at the fan face lowers the level of forward radiated fan noise from a supersonic inlet. The Modified inlet is, therefore, expected to provide a reduction in fan noise radiation at the test speed of 88PNC.

Table 1. Circumferential Direction of Mach number at the Fan Face

Inlet Configuration	Circumferential Distortion (88 PNC)	Circumferential Distortion (60 PNC)
Baseline Inlet	0.37	0.22
Modified Inlet	0.16	0.11
Reduction Factor	2.3	2.0

3.1.2 Inlet Throat Mach Numbers

In addition to affecting the generation of fan noise, properties of the inlet flow field are important for determining how the noise will propagate to the inlet openings. The Mach number at the throat region has a considerable effect on the noise propagation properties of a supersonic inlet. High inlet throat Mach numbers increase the time required for a noise signal to propagate to the inlet mouth, thereby dissipating more of the

signal energy. As discussed in section 2.3, this process of noise attenuation is referred to as the "choking effect" and is expected to occur for Mach numbers greater than 0.5.

The effect of fan speed on the throat Mach number is shown for the three inlet door combinations (Baseline, Modified, and auxiliary doors closed) in Figure 13. At the test speed of 88 PNC, the throat of the Modified inlet is choked while the Baseline inlet has a throat Mach number of 0.56. The large difference in throat velocity will give the inlets different acoustic properties. The choked throat of the Modified inlet is expected to attenuate the noise propagating to the front of the inlet. The throat of the Baseline inlet, with a Mach number only slightly greater than 0.5, is not expected to significantly reduce propagating fan noise.

The throat Mach number results for the closed door configuration are included to illustrate the need for auxiliary inlet doors during aircraft takeoff. The throat of the closed inlet chokes, that is reaches its maximum mass flow rate, at approximately 75 PNC. At 88 PNC, the engine will be unable to draw enough air to generate the thrust required for aircraft takeoff. The addition of auxiliary doors, either Baseline or Modified, prevents the inlet from choking before 88 PNC, and allows the engine to generate the required thrust.

3.1.2 Auxiliary Door Mach Numbers

To further investigate the effects of the modified door geometry on the inlet flow field, calculations were made to estimate the mass flow rates through the inlet throats and auxiliary doors of the two inlet configurations . In addition, estimations of the auxiliary

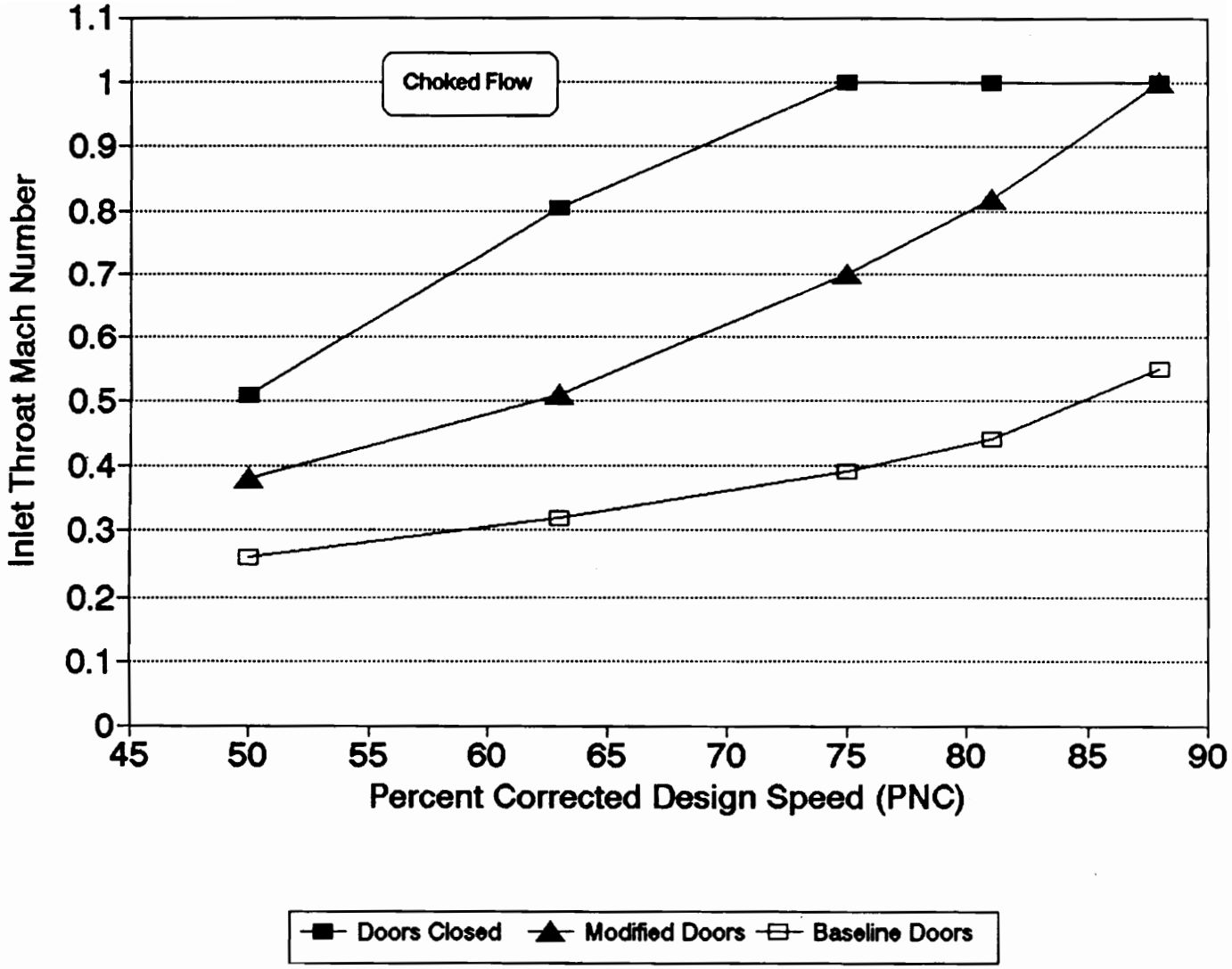

Figure 13. Inlet Throat Mach Number vs. Fan Speed

door Mach numbers were made to evaluate the effectiveness of the modified door design in employing the choking effect within the auxiliary door passage.

The mass flow rate values at the fan face, throat, and auxiliary door stations of the Modified and Baseline inlets for the test speed of 88 PNC are shown in Table 2. The fan mass flow rates were calculated from the corrected fan mass flow rate, given by the simulator performance map, and the area averaged total pressure at the fan face. The throat mass flow rates were calculated isentropically from the measured values of throat Mach number and the inlet throat area. To calculate the mass flow rates of the auxiliary doors, the throat mass flow rates were subtracted from the corresponding fan mass flow rates.

Table 2. Inlet Mass Flow Rates and Mach Numbers at 88 PNC

	Mass Flow Rate (lbm/sec)			Mach Number	
Inlet	Fan	Throat	Doors	Throat	Doors
Modified	2.33	1.79	0.54	1.0	0.39
Baseline	2.38	1.25	1.13	0.56	0.36

Although both inlets allow passage of approximately the same mass, the Modified inlet draws 52% less mass through the auxiliary doors than the Baseline inlet. This difference in auxiliary door mass flow rate is a result of the 50% smaller throat area of the Modified doors. The more restrictive Modified doors cause more air to be drawn through

the inlet throat, thus increasing the throat Mach number of the Modified inlet as illustrated in Figure 13.

The Modified doors were designed with a smaller throat area to increase the Mach number of the flow entering through the doors. Estimated values of Mach number in the Modified and Baseline doors are given in Table 2. The door Mach numbers were calculated isentropically from the door mass flow rates and the door throat areas (i.e., minimum cross-sectional area). The Modified door geometry provides only a 10% increase in auxiliary door Mach number over the Baseline geometry. In addition, the door Mach number of the Modified inlet is below 0.5, so that it is not expected that the choking effect will occur in the Modified doors. Therefore, the estimated door Mach number values indicate that employment of the choking effect in the converging door passage of the Modified auxiliary doors has not been achieved.

3.1.3 Inlet Aerodynamic Performance

The sharp cowl edge at the entrance of the inlet is expected to create a region of separated flow downstream of the cowl lip. The magnitude of the lip separation, expected to be greatest for static test conditions, is of interest for evaluating the aerodynamic performance of the inlets. The total pressure recovery profiles from the inlet lip station, shown in Figure 14, provide a good indication of the degree of lip separation occurring at the mouth of the inlet. The profile for the Modified inlet shows considerably more total pressure loss near the tip side of the passage than the Baseline profile. The larger degree

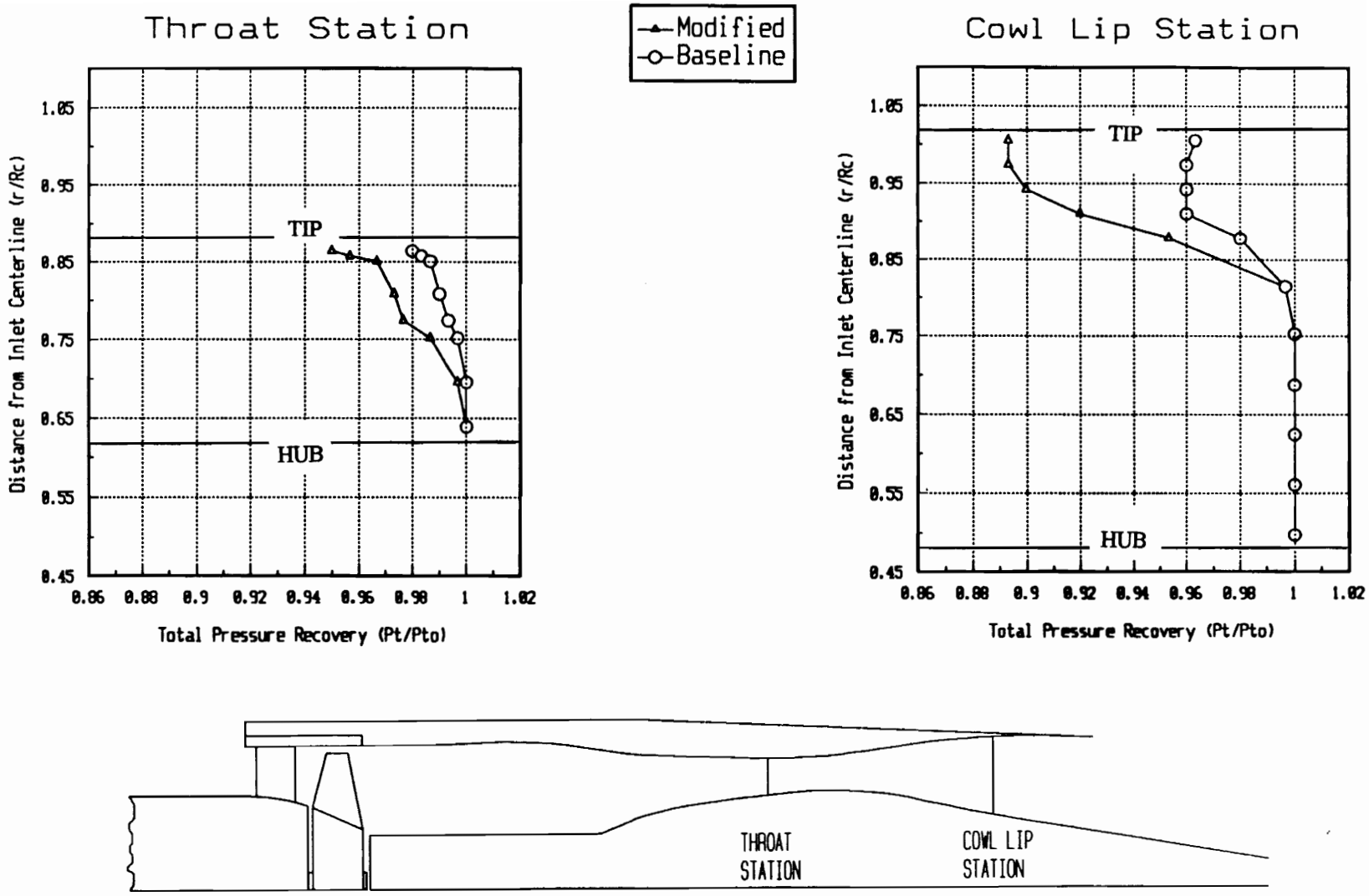

Figure 14. Total Pressure Recovery Profiles at the Cowl Lip and Throat, 88 PNC

of lip separation for the Modified inlet configuration is consistent with the fact that 43% more mass passes through the mouth of the Modified inlet than the mouth of the Baseline inlet. Both inlets show complete total pressure recovery in the region between the center of the passage and the hub wall.

The total pressure recovery profiles at the throat stations of both inlet configurations are also shown in Figure 14. The throat contours display a trend similar to the results of the cowl lip station. Near the tip wall, the total pressure in the Modified inlet is approximately 7% lower than that of the Baseline inlet. Again, both profiles show 100% total pressure recovery near the hub wall. The shapes of the throat profiles indicate that the higher-loss fluid from the cowl lip separation region remains near the tip wall as the air moves down the inlet. The profiles for both inlets show increased losses immediately next to the tip wall of the passage. The losses indicate the presence of a measurable boundary layer on the tip wall. The thickness of the boundary layer in the throat region of the Modified inlet is important in determining how much noise will "leak" past the choked throat due to the subsonic flow velocity in the boundary layer.

The overall aerodynamic performance of an inlet depends considerably on the average total pressure recovery at the exit plane of the inlet (fan face). The average total pressure recovery values for the Modified and Baseline inlets, given in Table 3, were calculated from the total pressure data at the fan face station from Figure 11. It is important to note that the total pressure measurement grid at the fan face station was originally developed to provide a measurement of inlet distortion and is somewhat cruder

than what would be required to provide a highly accurate measurement of inlet pressure recovery. The Baseline inlet configuration is shown to have a 2% advantage in total pressure recovery over the Modified configuration. Although it is difficult to determine the primary cause of the additional total pressure loss in the Modified inlet, there are several possible contributors: the larger degree of cowl lip separation, additional boundary-layer losses, shock losses at the sonic throat, and turbulent mixing of the auxiliary door flow (although the Baseline configuration would be expected to exhibit equal or greater mixing losses). A 2% reduction in total pressure recovery can represent a significant decrease in inlet performance. The decrease in performance for the Modified inlet would occur only during aircraft takeoff, however, when engine efficiency is not critical. The Modified inlet would not alter the engine efficiency and aircraft performance during supersonic cruise because the auxiliary doors are closed after takeoff.

Table 3. Average Total Pressure Recovery at Fan Face and Fan Exit

Inlet Configuration	Ptot Ave. Fan Face	Ptot Ave. Fan Exit	Pressure Ratio
Baseline Inlet	0.97	1.34	1.38
Modified Inlet	0.95	1.30	1.38

The fan pressure ratios for both inlet configurations are also given in Table 3. The fan pressure ratio is used in conjunction with the fan exit area to determine the operating point of the engine on the simulator performance map. It is important that the simulator operating points for both inlets are the same so that a difference between the radiated noise levels cannot be attributed to a difference in the simulator operating condition. Table 3 shows the fan pressure ratios of the Baseline and Modified inlets to be the same, confirming that the simulator operating conditions are the same for both inlet configurations (the fan speed for both inlets is 88 PNC). Nuckolls[17] also found the fan pressure ratios for the two test inlets to be matched (fan Pt ratio = 1.18) at the fan speed of 60 PNC.

3.2 Acoustic Results

The acoustic results are presented in three sections. In the first section, sample frequency spectra are used to illustrate various characteristics of the radiated noise. The second section presents the key results of the acoustic testing: the levels of the radiated noise for the Baseline and Modified inlets. A brief analysis of the generation, propagation, and radiation of noise modes in the supersonic inlets is outlined in the final section.

3.2.1 Narrowband Noise Spectra

Narrowband spectra are useful for illustrating the characteristics of the radiated engine noise. Each sample noise spectrum presented in this section represents the linear average of the frequency spectra of ten successive data sets. The averages were calculated to account for random fluctuations in the levels of the fan noise tones. For example, the blade passing frequency tone varied by as much as 8dB when testing with the fan operating at a constant speed. Tone fluctuation ,characteristic of acoustic studies of turbomachinery, is the result of natural aerodynamic fluctuations that are exacerbated by testing in static conditions. These aerodynamic fluctuations and their effect on the static, acoustic testing of aircraft engines is discussed further in section 2.4.

Figure 16 illustrates the effect of simulator fan speed on the noise signal radiated from the Baseline inlet to the 20° microphone position. At the lower fan speed, 60 PNC, the blade passing frequency tone (BPF) is seen to dominate the spectrum. The onset of

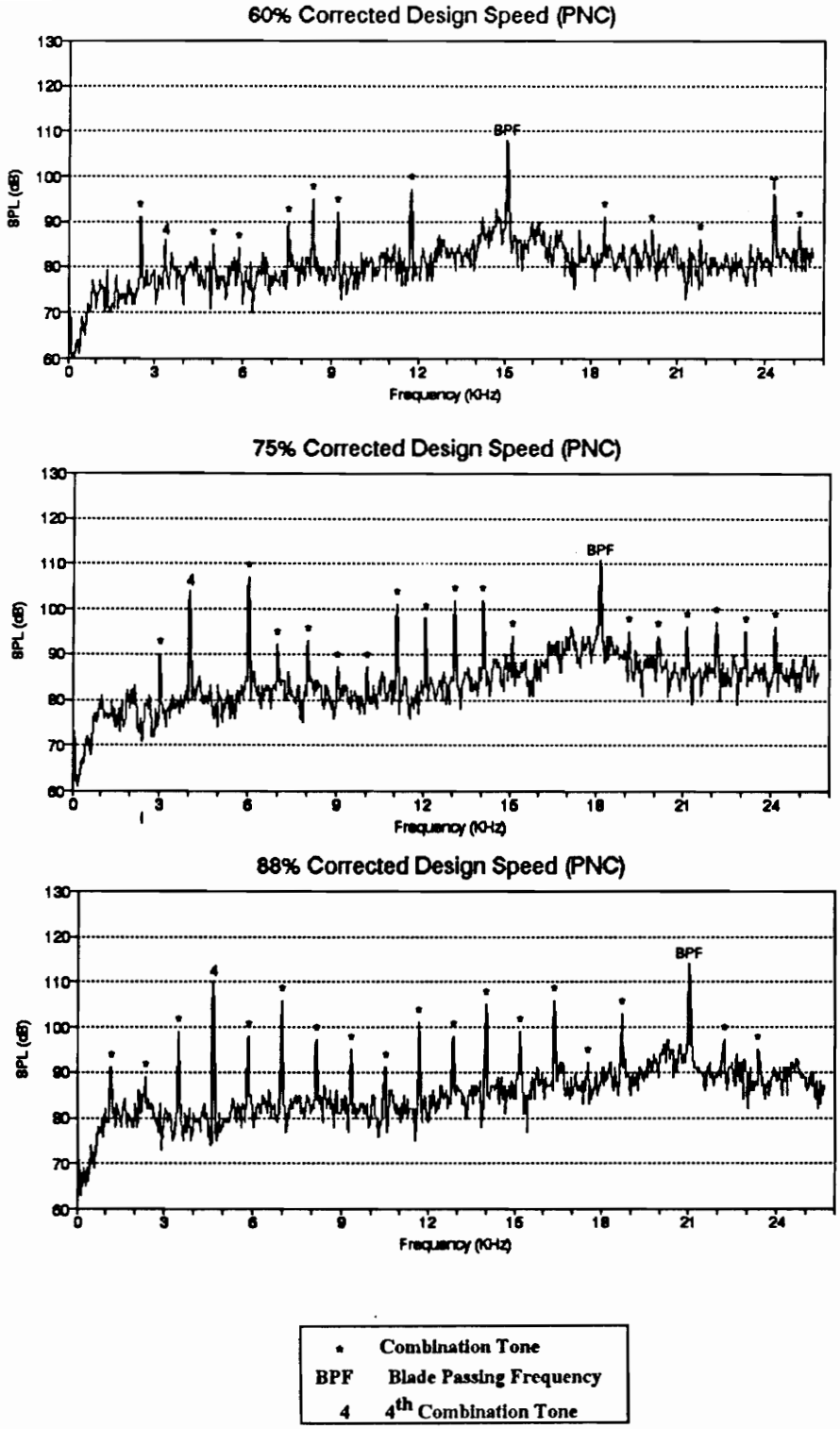

Figure 16. Effect of Simulator Speed on Radiated Noise, Baseline Inlet

combination tone noise is evidenced by the smaller tones located at integer multiples of the fan rotational frequency, 833Hz. Although the fan tip speeds are subsonic at 60 PNC, the regions of high axial air velocity at the fan face (see Figure 12, section 3.1.1) cause supersonic relative blade speeds which lead to the generation of combination tones. The tone located at a frequency equal to 29 times the rotational frequency of the simulator is the blade-passing signal of the 29-bladed drive turbine.

The sample noise spectra for the simulator speeds of 75 and 88 PNC show an expected increase in the level of the BPF tone. The increase in fan speed also results in a gradual increase in the abundance and magnitude of the combination tones; at 88 PNC, the noise spectrum contains combination tones at all multiples of the shaft frequency. A significant increase in the 4^{th} combination tone at the higher fan speed is also seen. The reason for the large magnitude of this tone is not known, although it is possibly the result of an interaction between the propagating combination tone shockwaves and the four centerbody support struts. The 4^{th} combination tone is also noted in the noise spectra of the Modified inlet and, to a smaller degree, the closed door configuration.

Sample spectra of the noise radiated to the 20°, 60°, and 110° microphone positions from the Baseline inlet are presented in Figure 17. These figures illustrate the changes in the radiated noise at different microphone positions. It is important to note the increase in the BPF tone level as the angular position of the microphone is increased. This trend, observed with both inlet configurations, will be further substantiated by the BPF tone radiation results of section 3.2.2. The higher level of the BPF noise signal in the

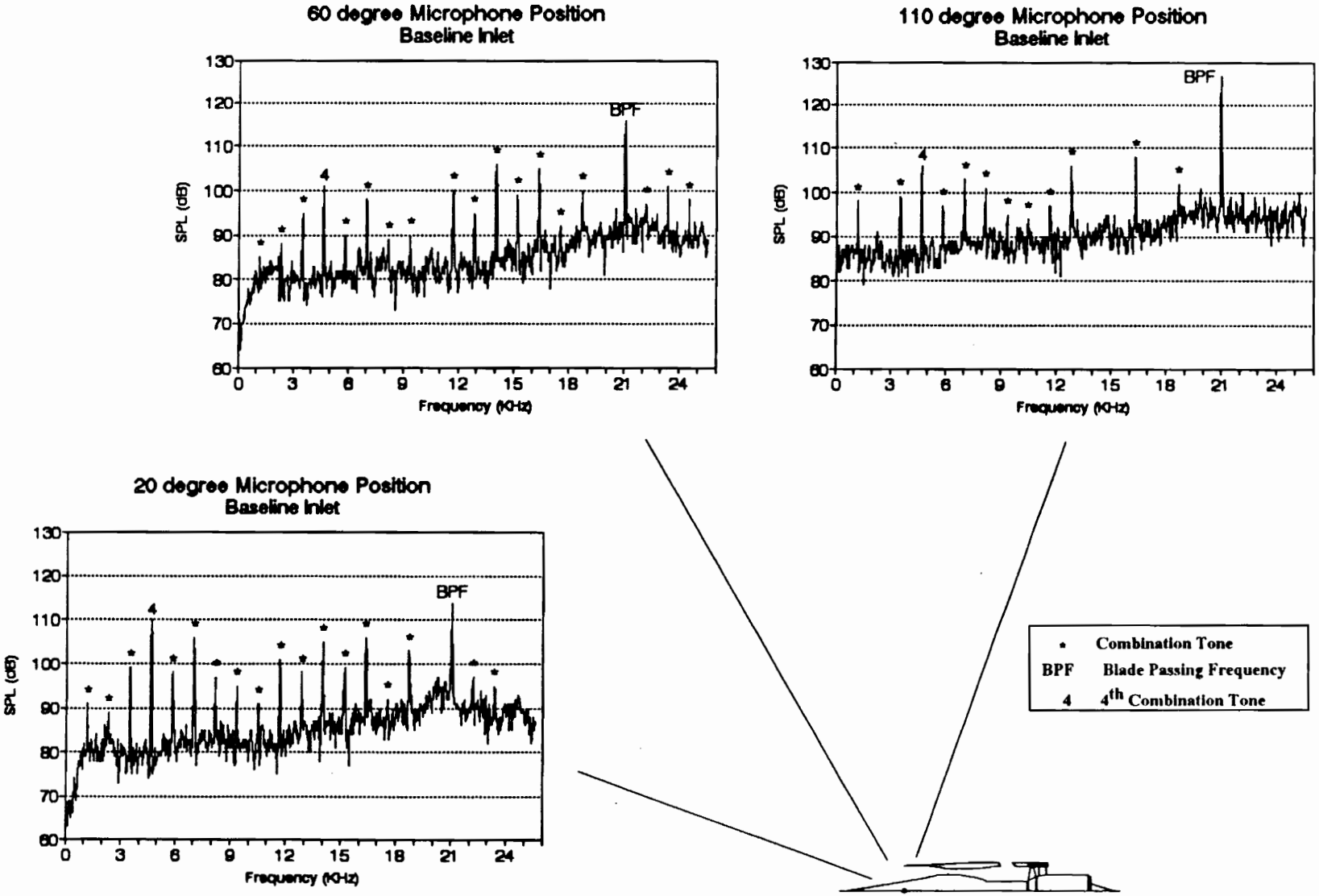

Figure 17. Radiated Noise Spectra at 88 PNC, Baseline Inlet

rearward sector of the measurement field is most likely due to the radiation of noise from the fan exit and auxiliary doors. The significance of the fan exit noise source to the measured radiation field is discussed further in the next section. Unlike the BPF tone, the magnitudes of the combination tones are not seen to change considerably with an increase in angular position, indicating that the noise radiating from the fan exit does not contribute to the level of the combination tone noise. This observation is consistent with the expectation that the shock waves which generate the combination tones will propagate from the fan blades in the upstream direction only (i.e., radiate from the doors and the inlet mouth, not from the fan exit).

The shape of the broadband noise (i.e., those frequencies between the distinct fan tones) also changes at the aft microphone positions. As the angular position of the microphone is increased from 20° to 110°, the broadband noise increases by roughly 4dB over most of the frequency range. For frequencies below 1000Hz, the broadband noise at the 110° location is approximately 15dB greater than the corresponding noise level at 20°. This low frequency noise present in the aft sector is believed to be generated by aerodynamic turbulence from the jet plumes of the fan and drive turbine.

Sample spectra of the noise radiated to the 20°, 60°, and 110° microphone positions from the Modified inlet are presented in Figure 18. A comparison of the noise spectra from the Modified inlet to the corresponding noise spectra from the Baseline inlet shows a reduction in BPF and combination tone levels. The reduction in the BPF tone noise for the Modified inlet is a key result of the acoustic testing that will be presented in

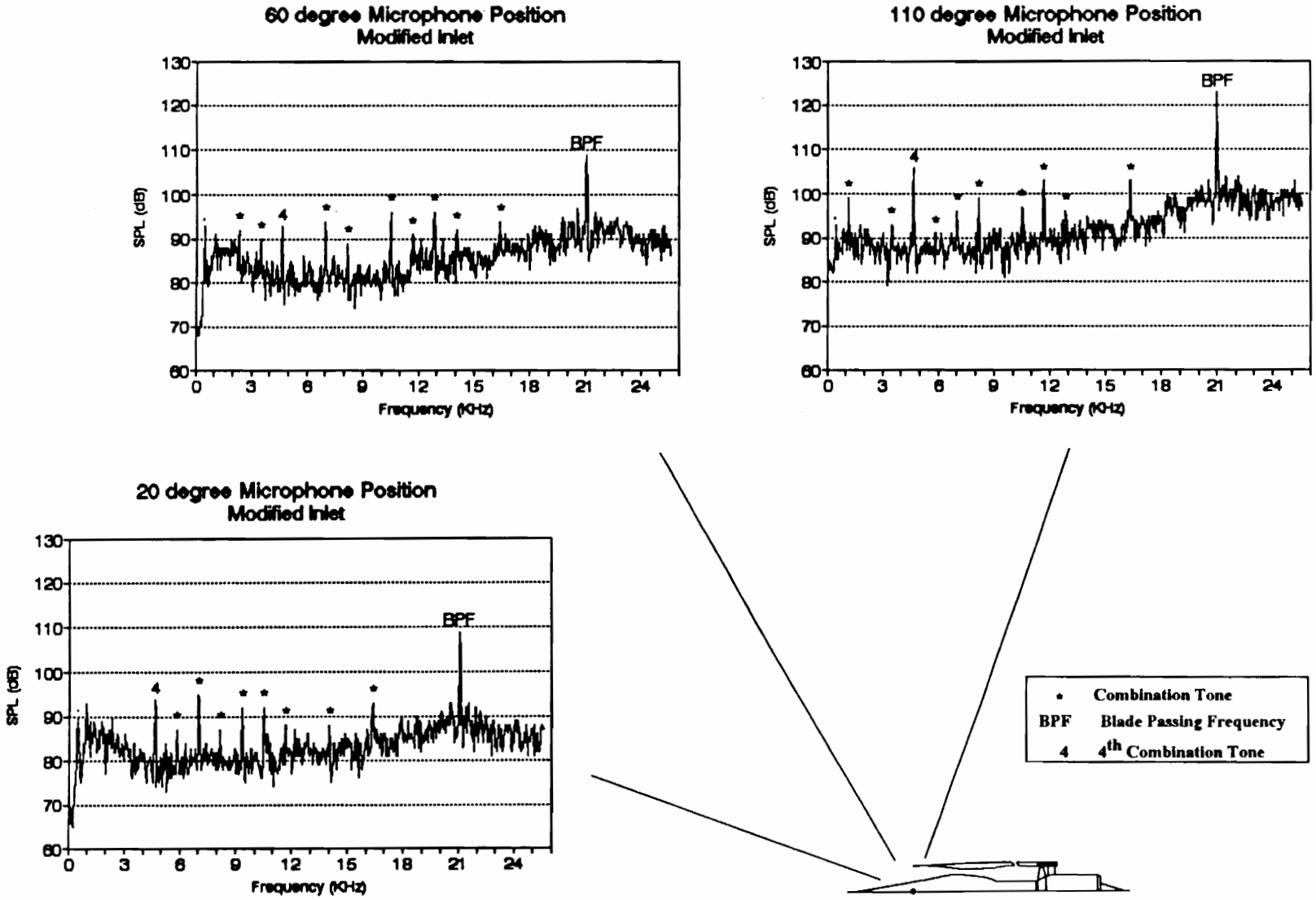

Figure 18. Radiated Noise Spectra at 88 PNC, Modified Inlet

detail in the next section. Although the reduction of the combination tones is also a significant result, it was not feasible in this experiment to measure the average of each combination tone in the spectrum. The contribution of the combination tones to the radiated noise is measured, however, in the overall noise results of section 3.2.2. The decrease in the magnitudes of the combination tones is most likely a result of a reduction in noise *propagation* due to the choked throat of the Modified inlet, and a reduction in noise *generation* caused by the different axial velocity distribution at the fan face station of the Modified inlet. The Mach number distribution at the fan face of the Modified inlet (Figure 15, section 3.1.1) shows lower axial Mach numbers in the region of the blade tips than the Mach number distribution for the Baseline inlet. A lower axial Mach number reduces the relative velocity of the fan blades, thereby reducing the strength of the shock waves that form the combination tones.

3.2.2 Radiated Noise Levels

This section presents the key results of the acoustic testing. A comparison between the fan noise radiation patterns of the Baseline and Modified inlets illustrates the improved acoustic performance of the Modified inlet. In addition, the noise radiation patterns of the inlets at different circumferential angles are presented to verify the acoustic performance of the Modified inlet at other points in the radiation field.

Figure 19 shows the level of the BPF tone at each microphone position for both inlet configurations. These results are also presented in a directivity plot format in Figure

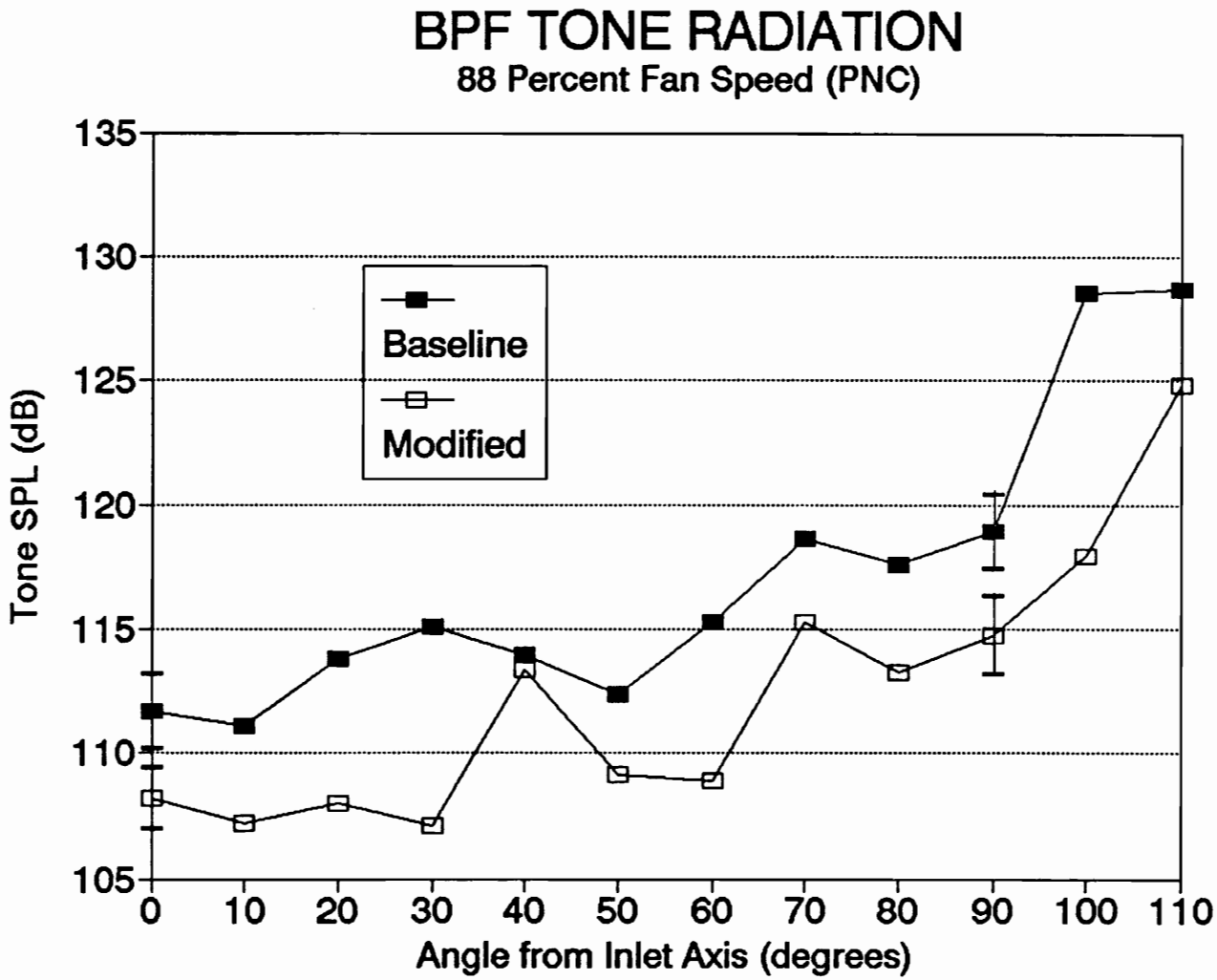

Figure 19. Radiation of BPF Tone, Baseline vs. Modified

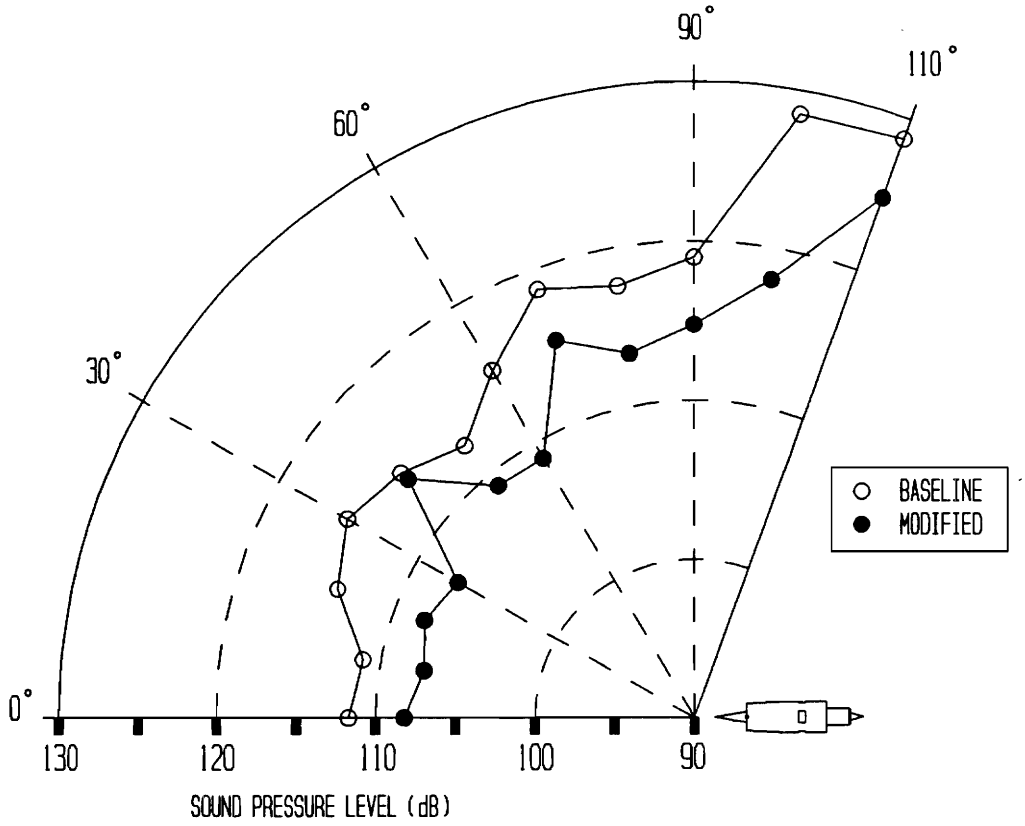

Figure 20. Directivity of BPF Tone, Baseline vs. Modified

20. Each BPF tone value represents the average of ten consecutive BPF readings from frequency spectra recorded with the signal analyzer. The two uncertainty bands shown in Figure 19, representing one standard deviation of the ten measurements taken at that angular position, indicate the magnitude of the BPF tone fluctuation. .

The Modified inlet provides an average reduction in the BPF tone of 4dB over the range of microphone positions. The largest noise reduction in the forward sector, 7dB, is seen to occur at 30°. At 40° the Modified inlet radiates BPF noise at essentially the same level as the Baseline inlet. Although the exact explanation for this point of relatively high radiation from the Modified inlet is not known, an analytical investigation into the possible fan noise radiation patterns of the inlets is presented in the final section of this chapter.

The overall noise radiation patterns of the two inlets are shown in Figure 21. A directivity plot of these results is given in Figure 22. The sound pressure level of the overall noise (OASPL) is a useful quantity for comparing the acoustic performance of the inlets because it includes the noise contributions of the combination tones and broadband noise along with that of the BPF tone. The uncertainty bands shown in Figure 21 represent the range of the microphone signal voltage recorded during measurements at that angular position. The voltmeter reading, used to calculate the overall noise data, was less influenced by aerodynamic fluctuations than the BPF tone levels recorded with the signal analyzer. This increased stability is reflected in the smaller size of the overall noise uncertainty bands.

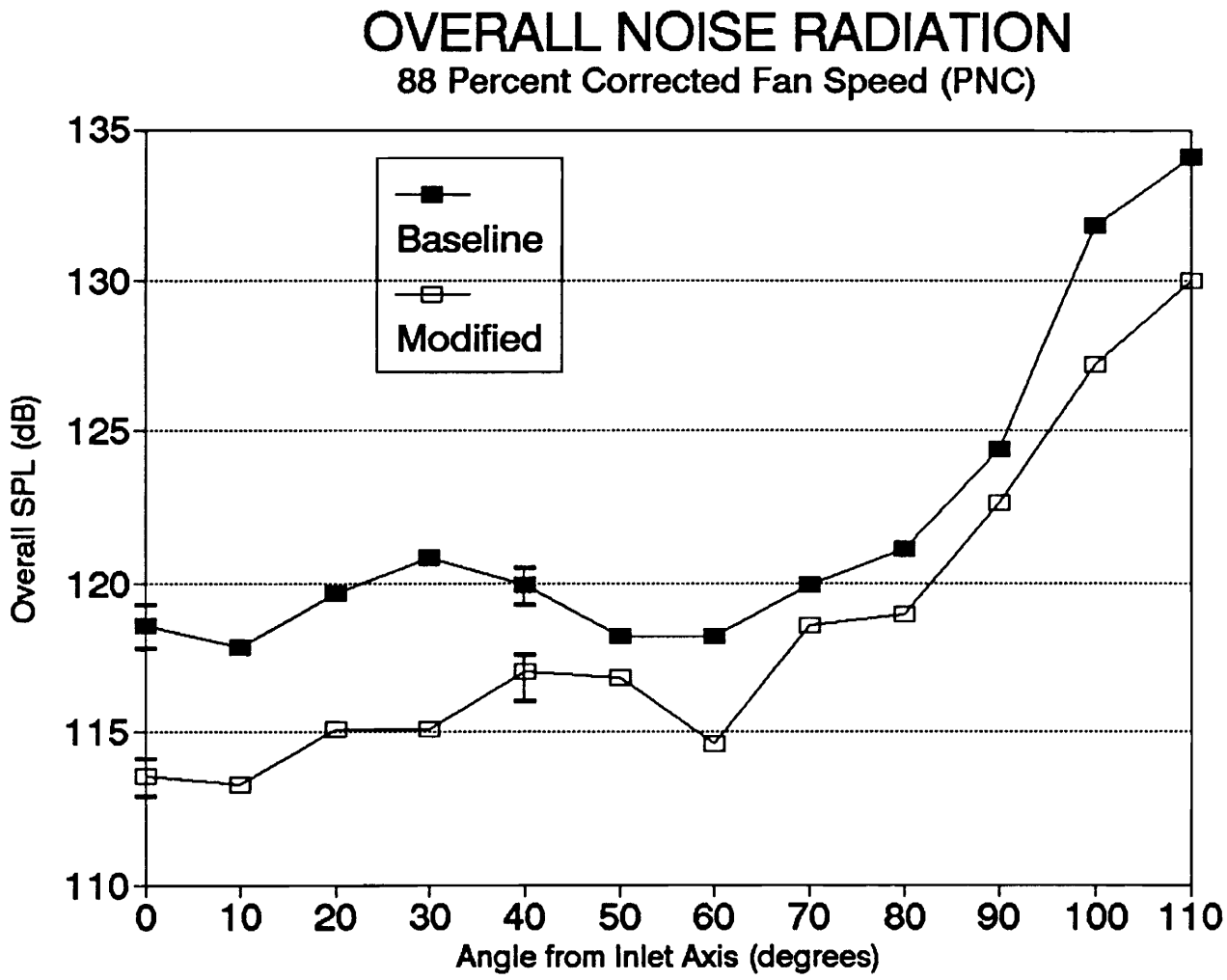

Figure 21. Radiation of Overall Noise, Baseline vs. Modified

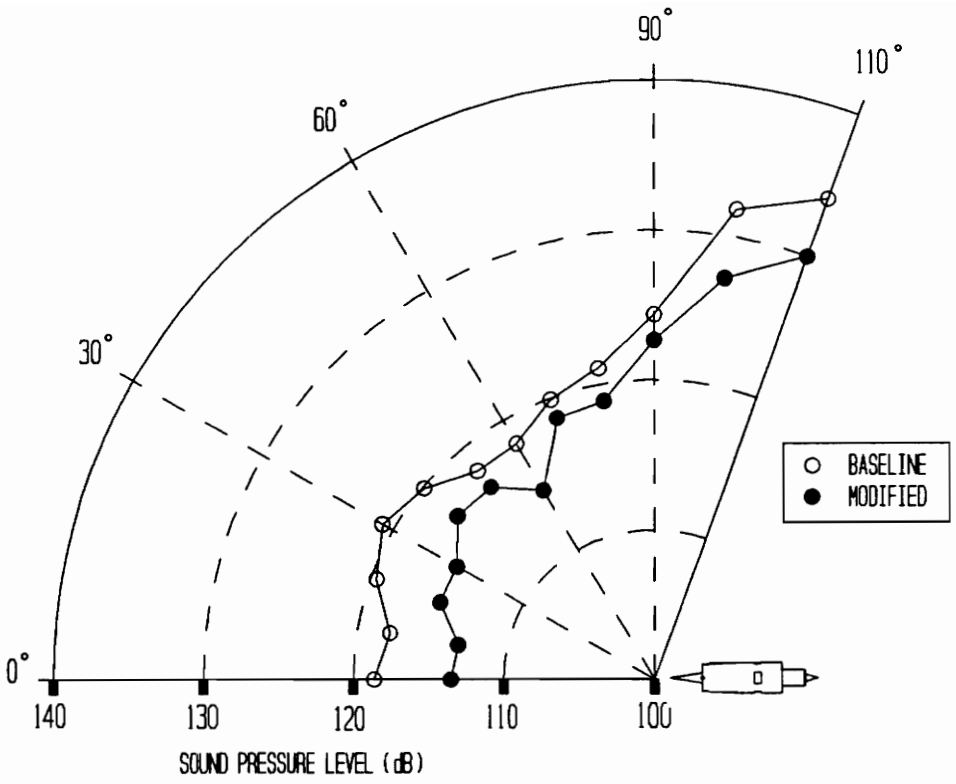

Figure 22. Directivity of Overall Noise, Baseline vs. Modified

The Modified inlet provides an average reduction in the radiated overall noise of 3dB(OASPL) over the range of microphone positions. The reduction in overall noise for the Modified inlet reflects both the lower levels of the combination tones and the reduction in the BPF tone.

The BPF tone and overall noise radiation plots for both inlet configurations show a trend of rising noise levels in the aft sector (90° to 110°), reflecting the contribution of the sound radiated from the fan exit. The noise radiated from the fan exit is expected to be of greater magnitude than that radiated from the inlet mouth because of the considerably shorter duct length between the fan and the fan exit (essentially the fan shroud only). A shorter duct length results in less attenuation of the noise as it propagates to the duct opening. The Modified inlet does show an improvement in acoustic performance over the Baseline inlet in the aft sector, indicating a reduction in the noise radiated from the fan exit for the Modified inlet.

The acoustic results presented thus far represent the noise radiated from the inlets to a single measurement plane. The radiation field surrounding the inlet is not expected to be completely axisymmetric, however, due to the potential for noise radiation through the auxiliary doors. For this reason, additional tests were conducted to verify the acoustic performance of the inlets at circumferential angles other than the primary test configuration. The procedures and results of the additional acoustic tests are presented in detail in Appendix A. For the primary test configuration, the microphone positions were arranged in a plane, parallel to the ground, that bisected the auxiliary inlet doors. To

measure the noise radiation at different circumferential angles, the inlet was rotated relative to the microphone measurement plane. The additional overall noise measurements were made at circumferential angles of 22.5° and 45° from the primary inlet orientation. The acoustic results from the additional measurement planes (Appendix A) show a reduction in noise radiation for the Modified inlet similar to that which occurred in the primary test orientation, although the magnitude of the reduction was slightly less in the aft sector of the additional planes. Thus it is expected that the Modified inlet will provide a reduction in radiated noise at all points in the forward radiation field.

Figure 23 shows a comparison of the Baseline BPF tone radiation patterns for simulator speeds of 88 PNC (current test) and 60 PNC (Nuckolls, [18]). In the radiation sector between 0° and 60°, the higher fan speed does not increase the level of the BPF tone considerably; the average increase in the 0° to 60° region is approximately 2dB. In the aft sector, however, the increase in tone level is considerable, particularly at 100° and 110°. The reason for the moderate increase in tone level in the forward sector is most likely a choking effect created by the higher throat Mach number at the 88 PNC fan speed; Nuckolls[18] measured a throat Mach number of 0.32 for the fan speed of 60 PNC, while the throat Mach for the current test is 0.56. The significant increase in tone level in the rear sector occurs because noise radiated from the fan exit increases with fan speed and is not affected by the increase in throat Mach number. The shapes of the radiation patterns at the two fan speeds differ considerably because the radiation direction of each noise mode depends on the frequency of the noise, which increases proportionally with fan

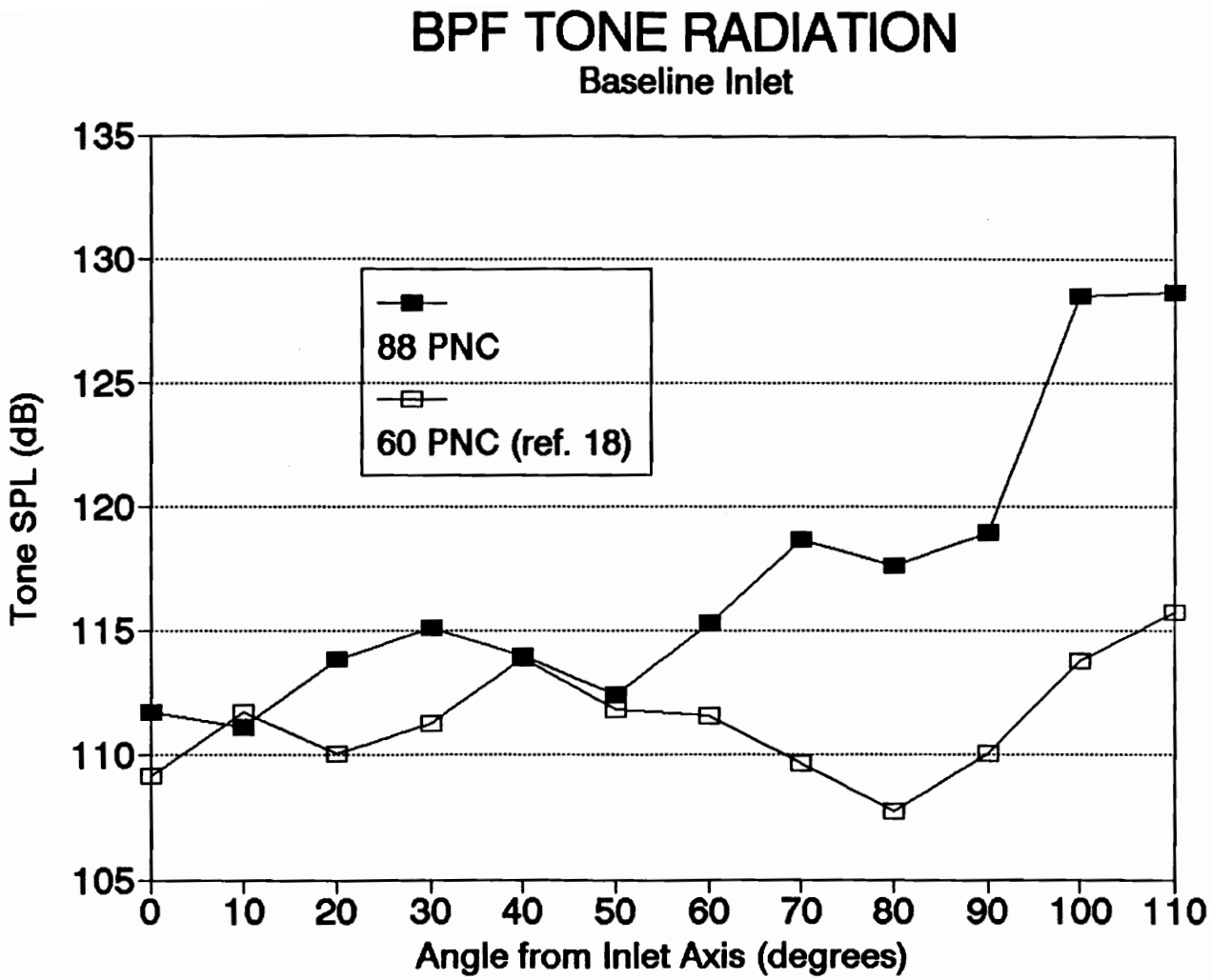

Figure 23. Radiation of BPF Tone at 60 and 88 PNC, Baseline Inlet

speed. The next section discusses the radiation patterns of the individual noise modes in detail.

3.3 Analysis of Radiation Patterns

The theory of fan noise generation and propagation in circular ducts developed by Tyler and Sofrin [13] is used here to determine the fan noise mode orders of the fundamental BPF tone which radiate from the supersonic test inlets. In addition, the approximate angular positions of the primary lobes of the radiation patterns of the modes are calculated and compared to the experimental results. The theory of modal generation and propagation is reviewed here only briefly; references [13] and [14] should be consulted for a comprehensive derivation.

3.3.1 Generation of Pressure Modes

The BPF tone noise is generated by the interaction of the rotating fan blades with stationary (relative to the fan rotation) flow disturbances. In the analysis of Tyler and Sofrin[13], the fan noise signal is represented by a superposition of spinning pressure distributions of n lobes and m radial orders propagating along the axis of the passage. The circumferential order (i.e. number of lobes) of a particular rotating pressure pattern is determined by the number of rotating blades, B, and the number of stationary disturbances, V:

$$n = B - kV \qquad k = \pm 1,2,3... \qquad [3.1]$$

In the current supersonic test inlets, there are three apparent sources of evenly spaced circumferential distortion near the fan: the row of stator blades behind the fan (order V = 26), the four centerbody support struts (order V = 4), and the auxiliary inlet doors (order V = 4). By equation [3.1], it is possible for each of the disturbance sources to generate an infinite combination of modal patterns. There is, however, a finite set of modal patterns that can actually propagate in the inlet duct.

3.3.2 Propagation of Pressure Modes

The axial propagation of the generated noise modes is determined by the axial wave number, K_{nm}:

$$K_{nm} = 2\pi/c\ (f^2 - f_{nm}^2)^{0.5} \qquad [3.2]$$

In this equation, **f** is the frequency of the noise signal , in this case the BPF tone, and f_{nm} is the cutoff frequency for the (n,m) mode. It has been demonstrated by [13] that the amplitude of the noise will decay rapidly in the duct if the axial wave number has an imaginary value (i.e., $f_{nm} < f$). This condition is referred to as "cut-off." In order for a mode to propagate through the duct, the cut-off frequency of the mode must be below the noise frequency. For the annular passage of the supersonic inlet, the cut off frequency of each mode is determined by the zero-pressure-gradient constraints at the inlet hub and tip walls. A linear combination of the frist and second order Bessel functions, typically refered to as the E-function, is required to satisfy these boundary conditions. The cut-off frequency of each mode is dependant upon the radial and circumferential order of the

pressure pattern, the outer radius of the duct, and the hub/tip ratio of the passage. As an alternative to using E-functions for determining the cut-on noise modes, Tyler and Sofrin[13] have tabulated the critical tip Mach numbers for several circumferential mode orders (lowest radial order). For a particular pressure pattern and hub/tip ratio, there is a minimum Mach number at which the lobe tips must rotate in order to be cut-on. Table 4 presents the circumferential mode orders which are cut-on in the supersonic inlet. Two locations along the inlet passage were evaluated for the cut-on criteria: the fan face (hub/tip = 0.38), and the inlet throat (h/t = 0.75). For the lower circumferential-order modes, the actual tip Mach numbers are well above cut-off and several radial mode orders above the fundamental are expected to be cut-on. For the circumferential mode m = 14, the actual tip Mach number is just above cut-off so that all radial modes above the fundamental will be cut-off.

Table 4. Cut-on Modes in the Supersonic Inlet

		Circumferential Mode Order, m				
		2	6	8	10	14
Fan face h/t = 0.38	Actual M_{tip}	10.0	3.3	2.5	2.0	1.4
	Critical M_{tip}	1.4	1.3	1.2	1.2	1.2
Throat h/t = 0.75	Actual M_{tip}	9.1	3.0	2.3	1.8	1.3
	Critical M_{tip}	1.2	1.1	1.1	1.1	1.1

3.3.3 Radiation of Pressure Modes

Each of the modal patterns that reach the inlet mouth can be expected to radiate to the far-field to form a radiation pattern comprised of lobe-shaped amplitude variations. Homicz and Lordi [14] developed a simplified method for determining the approximate angular location of the primary lobe of a radiation pattern from an unflanged circular duct. Although the inlet evaluated here is an annular duct, numerical evaluations by [14] have indicated that for hub/tip ratios less than 0.5, the radiation pattern is roughly approximated by circular duct predictions. Table 5 gives the angular positions of the primary lobes of the modal patterns listed in Table 4.

Table 5. Primary Lobe Radiation Angles of the Cut-on Modes

	Circumferential Mode Order, m				
	2	6	10	8	14
radiation angle	8.2°	20.5°	26.8°	33.7°	51.3°

A comparison of the radiation angles in Table 5 with the BPF directivity plot of Figure 20 indicates the possibility of a primary lobe in the 30° to 40° region. The pattern for the Baseline inlet shows a broad-lobed shape centered on 30°, while the pattern for the Modified inlet shows a narrower lobe at 40°. This general region corresponds to the

primary lobe locations of the following circumferential mode orders: m = 10, 14 (lowest radial order). The m = 10 mode is generated by the rotor-stator interaction, while the m = 14 mode is generated by the flow disturbances of the support struts or auxiliary doors. It would also be possible for the higher order radial modes of the m = 2, 6, and 8 circumferential order modes to radiate to the 30° to 40° region. Because the analysis of [13] does not account for the relative amplitudes of the noise modes, it is not possible to identify a particular mode as the primary source of BPF noise.

There are limitations to the previously outlined analysis of modal propagation and radiation. Primarily, the analysis does not account for the presence of mean flow in the duct. The effect of uniform mean flow has been addressed by Sofrin and McCann[18], but the analysis has not been extended to axially-dependent mean flow velocity as is the case with the supersonic test inlets. Mean flow in a direction opposing propagation effectively increases the cut-off frequency, so that fewer modes are actually expected to propagate to the inlet mouth than are shown in Table 5. In addition, the changing duct radius of the supersonic inlet does not conform exactly to the analytic model of uniform annular shape. Finally, it is important to realize that the measured radiation field shown in Figure 19 represents the combination of the radiation patterns of the inlet mouth, auxiliary doors, and fan exit. This superposition of radiation patterns makes the observation of distinct lobed patterns unlikely.

In section 3.2.3, the noise radiated from the exit of the fan was suggested as a likely cause for the higher noise levels in the aft measurement region. Unfortunately, the

short length of the fan shroud makes the analysis methods of [13] inapplicable to the noise radiated from the fan exit. For a noise frequency of 21kHz (the fundamental BPF at 88 PNC), the distance from the fan to the duct exit is less than one wavelength and it is likely that cut-off modes would be able to propagate to the opening. A ray method would be more appropriate to the analysis of the noise radiated from the fan exit, but not enough information is known about the effect of the stator row and fan mean flow to enable such analysis.

4.0 Conclusions and Recommendations

4.1 Conclusions

The principle objective of this research was to evaluate the aerodynamic and acoustic performance of a supersonic inlet with modified auxiliary inlet doors under simulated aircraft takeoff conditions. A small-scale model of an axisymmetric, mixed-compression, supersonic inlet was tested in conjunction with a 10.4cm (4.1 in) diameter turbofan simulator. Two auxiliary inlet door geometries were evaluated: a baseline geometry representative of current door designs, and a modified geometry designed to reduce inlet flow distortion and fan noise radiation.

Through improved distribution of the auxiliary door airflow, the modified door geometry provided a factor of 2.3 reduction in circumferential flow distortion compared to the baseline door configuration. Along with improved flow distribution, the modified doors were designed to employ the choking effect in the auxiliary door passages. Estimations of the auxiliary door Mach numbers showed that the choking effect in the modified doors was not achieved.

The modified doors demonstrated improved acoustic performance by lowering both the BPF tone and overall noise an average of 4dB(SPL) in the forward and aft sectors (0° to 110°). In addition to the primary test configuration, the improved acoustic performance of the modified doors was also verified at other circumferential planes in the measurement field.

Unfortunately, the improvements in acoustic performance and inlet distortion are accompanied by a decrease in inlet aerodynamic performance; the modified doors reduce the average total pressure recovery of the inlet by about 2%. It is felt, however, that a reduction in inlet pressure recovery of this magnitude during aircraft takeoff will not adversely affect the performance of the aircraft.

In conjunction with the results of Nuckolls and Ng[17], the results of this research have shown that the modifications made to the auxiliary door geometry will reduce forward-radiated noise during aircraft takeoff and landing approach, and consequently will lower the impact of a supersonic transport on aircraft community noise.

4.2 Recommendations

From the results presented in this paper and the previous work by Nuckolls[17], it is apparent that improvements to the design of a supersonic inlet can be realized through the use of a small-scale test program. Even more importantly, the small-scale test program provides a stage for low cost experiments to develop a better understanding of

the complex relationship between inlet aerodynamics and engine acoustics. Along this vein, there are several areas of research that warrant investigation with the test program. The noise spectra from the Baseline and Modified inlets showed the 4^{th} combination tone to be almost as significant as the BPF tone during aircraft takeoff. It was postulated that the large magnitude of this tone was the result of an interaction between the combination tone shock-waves and the four centerbody support struts. An investigation into the generation of this tone should be made so that it can be reduced with future inlet designs.

In addition to particular tones in the noise spectra, the radiation patterns of the inlets are also not fully explained. The analytical investigation into the radiation patterns of the theoretical fan noise modes was inconclusive due to the complicated superposition of the radiation patterns from the inlet mouth, doors, and fan exit. The acoustic baffle test of Appendix B suggests a method for individual examination of the radiation patterns of each noise source. Experiments conducted using an acoustic baffle for source isolation should provide results that can be more readily compared to analytical radiation patterns.

For these and other acoustic experiments, it will be important to establish a simpler method of acoustic measurement. A large number of data sets were averaged to acquire the current acoustic results for the BPF tone radiation. The extensive number of readings were required to provide adequate confidence in the results due to the fluctuating behavior of the BPF tone. Investigative research into BPF tone phenomena was limited by the daunting number of readings required to establish reliable trends. In comparison to the BPF data which were recorded with the signal analyzer, the overall noise measurements

made with the RMS voltmeter provided more stable readings and a simpler test procedure. The increased stability of the RMS meter data is probably due to the continuous nature of the signal measurement; the signal analyzer used 0.015sec. long samples of the microphone signal to generate each frequency spectrum and required many readings to resolve the random variation of the BPF tone. The RMS meter could be used to measure the BPF tone through the use of a narrow band-pass filter set to window the blade passing frequency. By using the RMS meter to measure the BPF tone, the acoustic tests could be simplified to allow for more exploratory research into the acoustic properties of the inlets. A signal analyzer would still be required, however, to provide the narrowband noise spectra.

Appendix A Additional Acoustic Measurements

The acoustic results presented in Figures 19 through 22 (section 3.2.2) represent noise radiated from the inlets to a single measurement plane. The radiation field surrounding the inlets is not expected to be completely axisymmetric, however, due to the potential for noise radiation through the auxiliary doors. For this reason, additional tests were conducted to verify the acoustic performance of the inlets at circumferential angles other than the primary test configuration. The microphone positions for the primary configuration were arrayed in a plane, parallel to the ground, that bisected the auxiliary doors. To measure the noise radiation at different circumferential angles, the inlet was rotated relative to the microphone measurement plane. This process is illustrated in Figure 23. The additional overall-noise measurements were made at angles of 22.5° and 45° from the primary inlet orientation. Figure 24 illustrates the effective microphone locations of the additional test configurations.

The overall noise levels radiated from both inlets to the 0°, 22.5°, and 45° circumferential angles are shown in Figure 25. For the Baseline inlet, the noise radiated to the aft region (70° and 90°) in the 0° circumferential orientation is 1 to 2dB greater than the corresponding noise levels for the 22.5° and 45° circumferential orientations. The higher noise level in the 0° orientation may be the result of direct noise radiation through the Baseline doors to the 0° measurement plane. The Modified inlet provides a reduction from the Baseline inlet noise levels at all measurement locations, although the magnitude

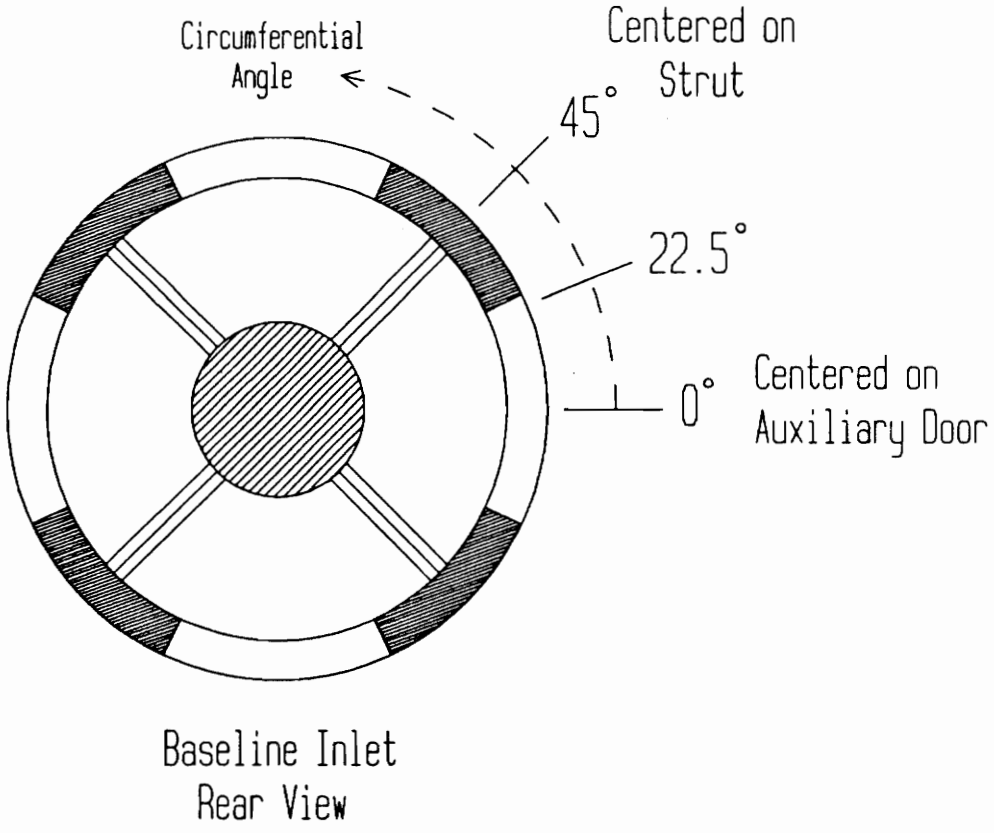

Figure 23. Circumferential Positions of Microphone Measurement Planes

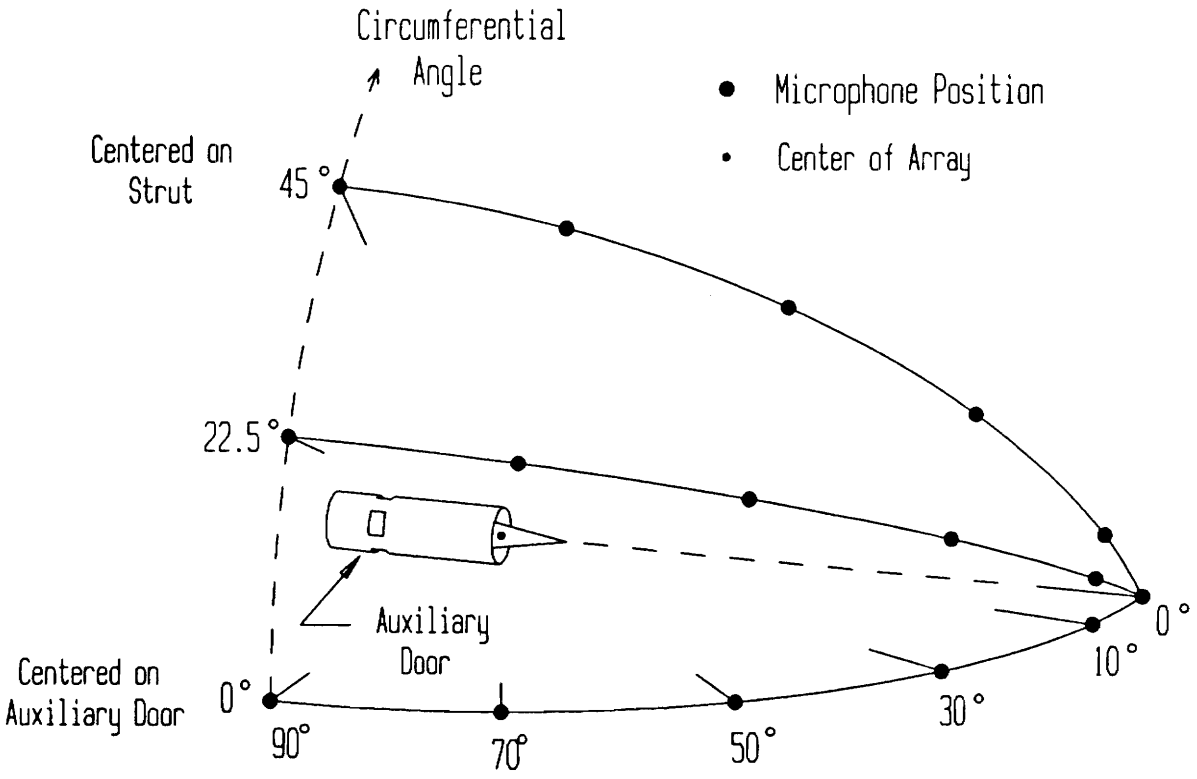

Figure 24. Effective Microphone Positions: 0°, 22.5°, and 45° Inlet Orientations

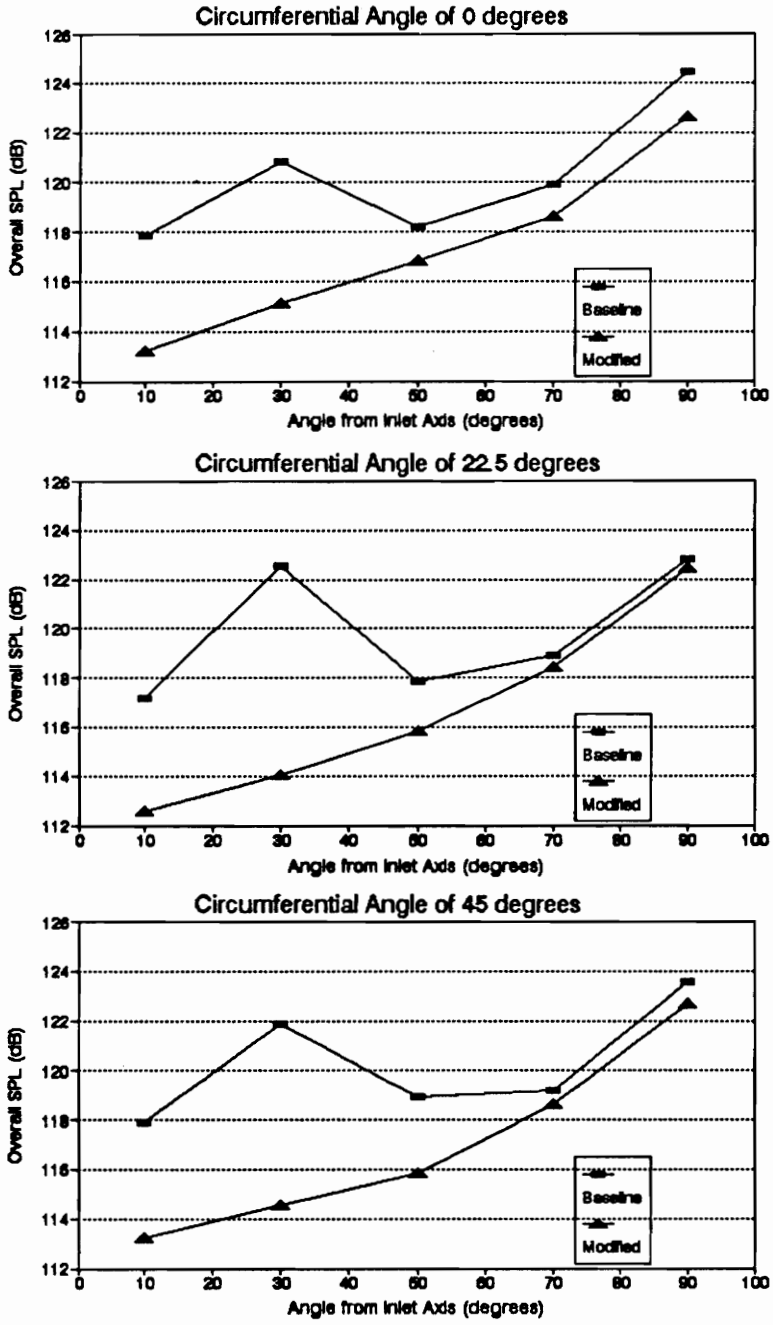

Figure 25. Radiation of Overall Noise: 0°, 22.5°, and 45° Inlet Orientations

of the reduction is only about 1dB for the aft (70° and 90°) microphone positions in the 22.5° and 45° circumferential orientations.

The noise reduction provided by the Modified inlet is further illustrated by the SPL contour plots in Figure 26. The symmetry of the auxiliary door construction was utilized to extend the 0° through 45° measurement grid (as illustrated in Figure 24) to the 360° contour plots shown. From the results of the additional acoustic tests, it is expected that the Modified inlet will provide a reduction in radiated noise at all points in the forward sector.

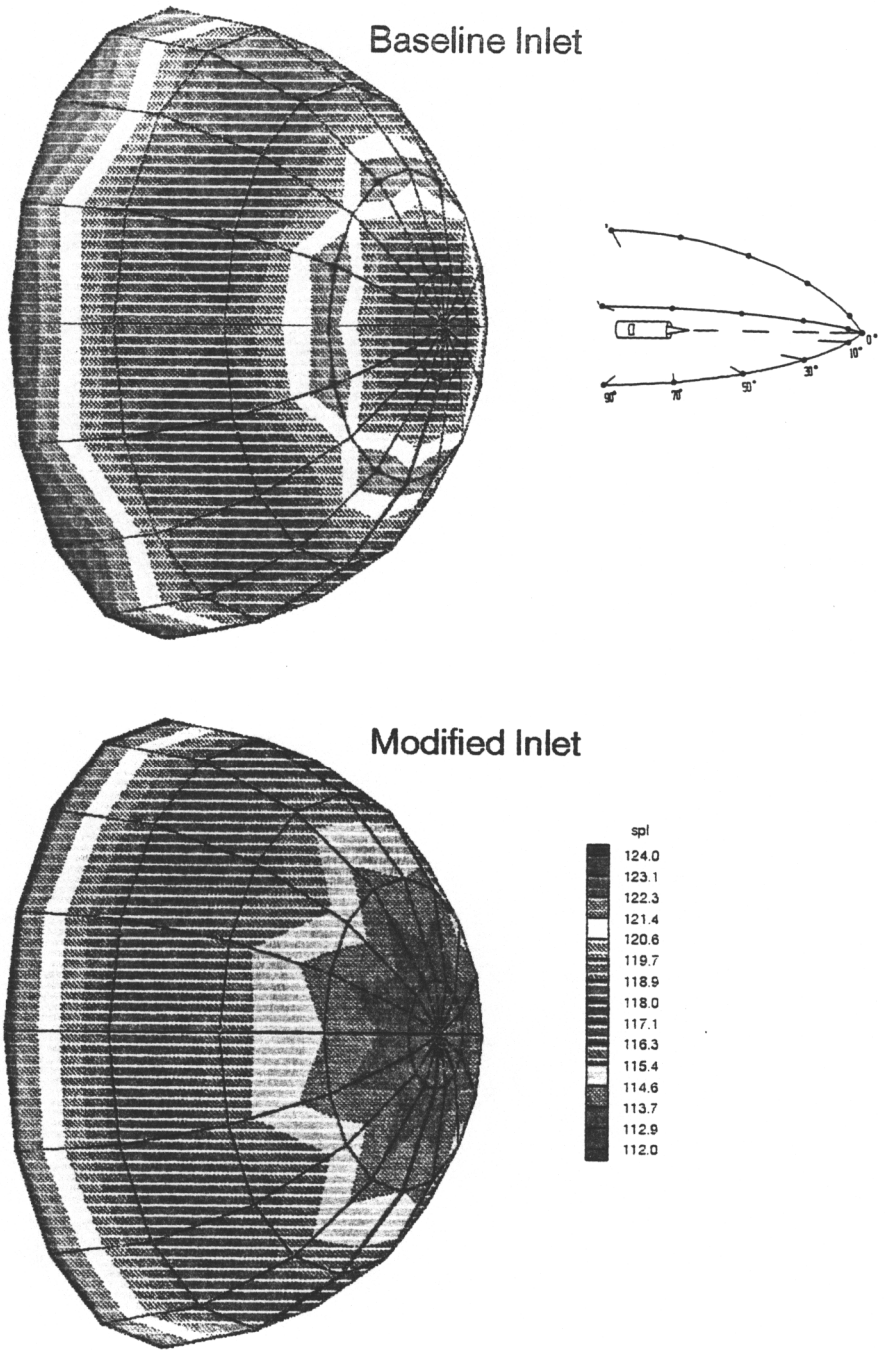

Figure 26. Overall Noise Contours, Baseline vs. Modified

Appendix B Closed Auxiliary Door Test

As discussed in section 2.3, the closed auxiliary door configuration which will be referred as the Closed inlet was accomplished by covering the Modified auxiliary doors with a 0.25 inch thick aluminum band. The resulting reduction in capture area caused the Closed inlet to reach the point of choked flow at a fan speed of approximately 70 PNC, illustrated by the Mach number plot of Figure 27. At fan speeds above 70 PNC, a normal shock is expected to form slightly downstream of the throat of the Closed inlet, creating shock losses that lower the aerodynamic performance of the inlet.

The total pressure distribution at the fan face station of the Closed inlet is shown in Figure 28 for the simulated-takeoff test speed (88 PNC). The combination of the separated flow at the cowl lip and the shock losses result in an average total pressure recovery of approximately 80%; a considerable decrease in performance from the 97% and 95% total pressure recovery values for the Baseline and Modified inlets. Although the throat of the Modified inlet is also choked at takeoff speed, the shock losses are minimal because the inlet throat just reaches the point of choking at 88 PNC. The high shock losses of the Closed inlet indicate that it is important to design the auxiliary doors so that the inlet throat will just choke at the maximum engine speed required for takeoff, thereby avoiding poor inlet performance due to excessive shock losses.

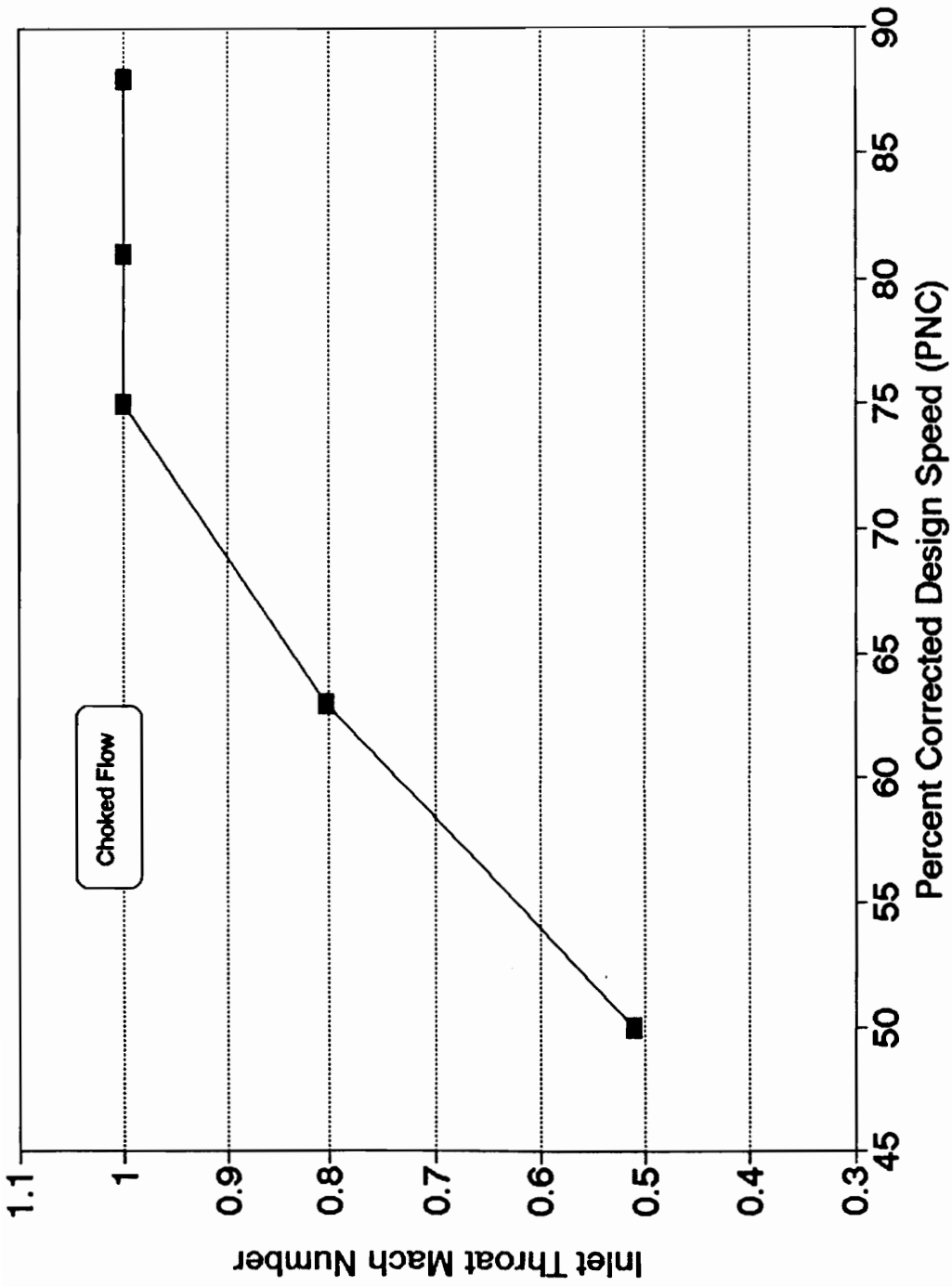

Figure 27. Effect of Simulator Speed on Throat Mach Number, Auxiliary Doors Closed.

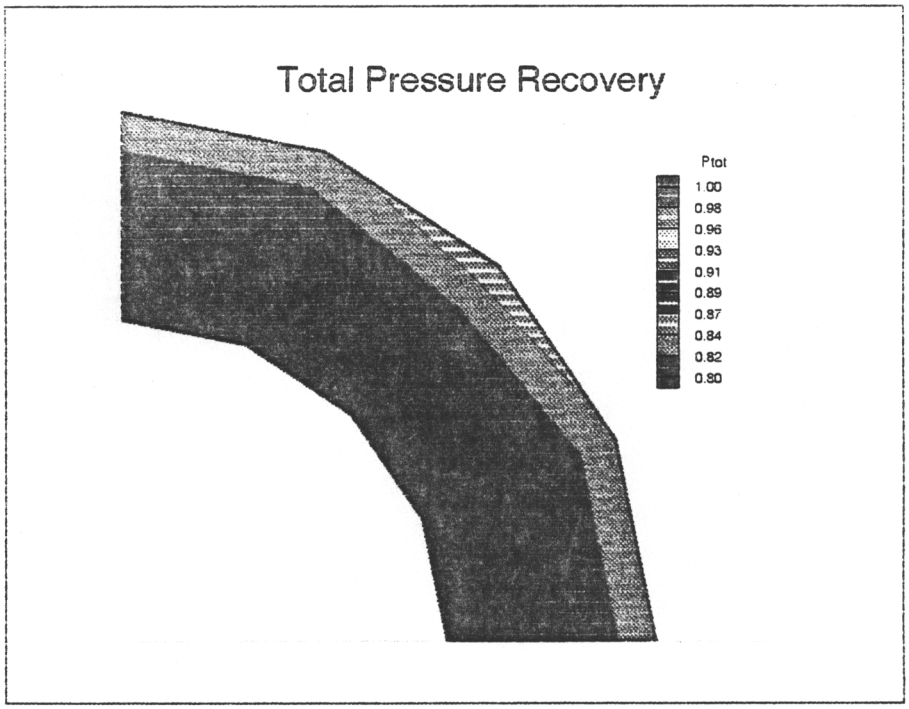

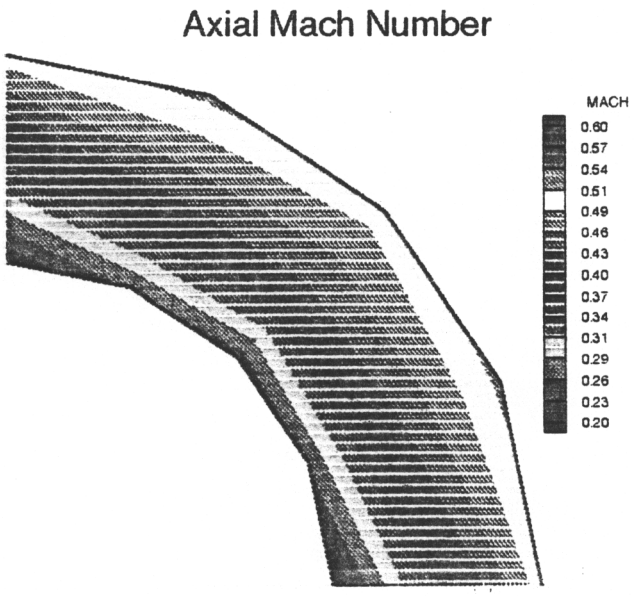

Figure 28. Total Pressure and Axial Mach Number Distributions at the Fan Face, Auxiliary Doors Closed

The axial Mach number contour plot for the Closed inlet, also shown in Figure 28, contains little circumferential distortion, reflecting the fact that there are no auxiliary doors to disrupt the axisymmetric nature of the inlet flow field.

Although the closed-door acoustic results were thought to be of value to provide additional comparisons to the Modified and Baseline inlet results, the Closed inlet configuration could not provide enough air flow to meet the requirements of the simulator at the simulated takeoff engine speed. Because the operating conditions of the simulator were changed considerably, the acoustic results for the closed inlet cannot be directly compared to the acoustic results from the Modified and Baseline inlets.

Sample spectra of the radiated noise are shown in Figure 29. At each angular position, the magnitude of the BPF tone is at least 4 dB less than the corresponding value for the Modified inlet (Figure 18, section 3.2.2). The decrease in the BPF tone is a result of the reduction in flow distortion and the absence of the auxiliary doors as a path for noise radiation. The noise spectra for the Closed inlet also display few combination tones; a result of the low axial Mach number at the fan face and of the choked inlet throat. Unlike the BPF and combination tones, the broadband noise is increased (particularly below 6kHz) from the Modified inlet results. The reason for the increase in broadband is not known, although it is possible the fan generated a higher level of broadband noise due to the low total pressure at the fan entrance. Similar to the results of the Baseline and Modified inlets, the Closed inlet noise spectra show increased BPF tone in the aft sector, reflecting the noise radiated from the fan exit.

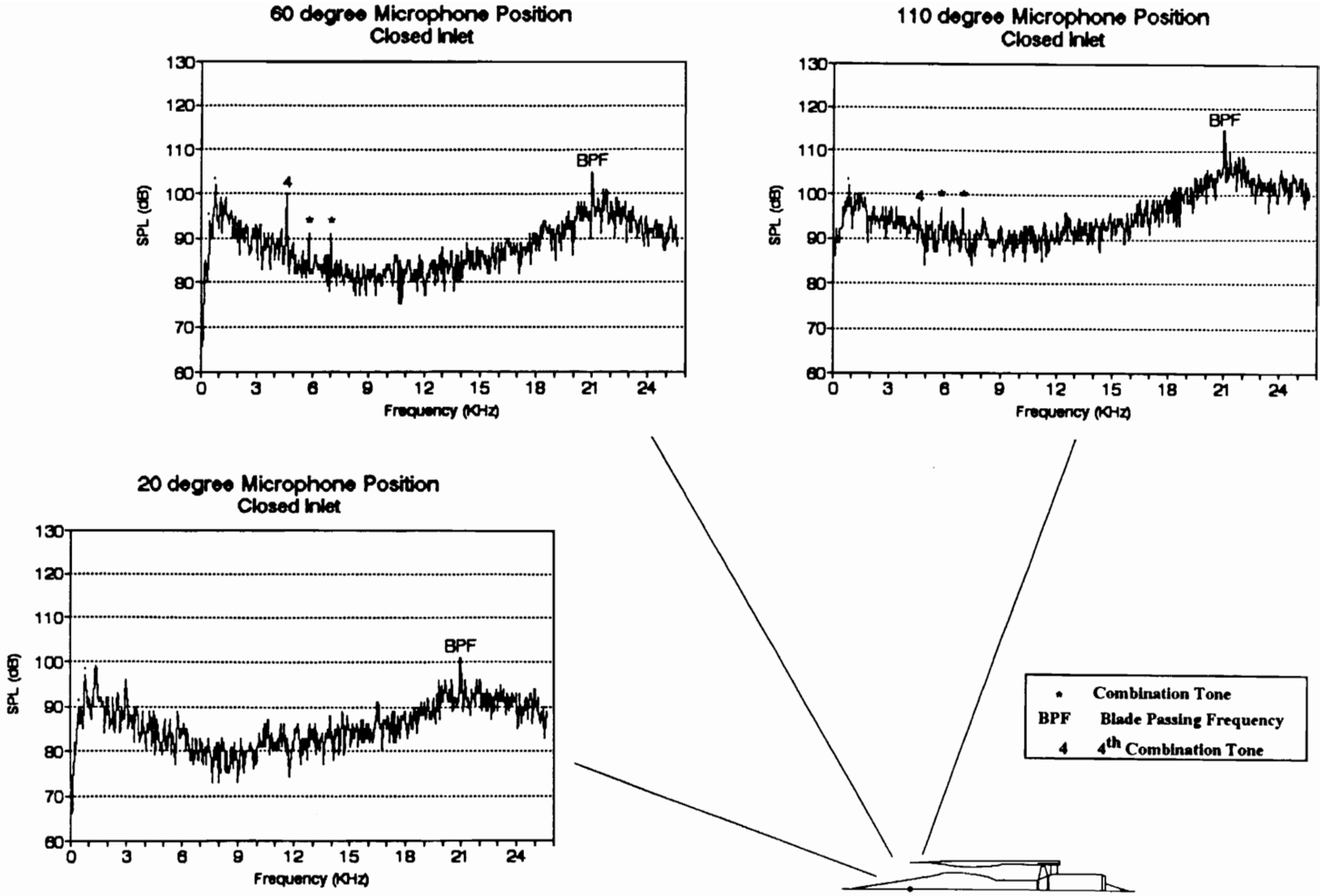

Figure 29. Radiated Noise Spectra at 88 PNC, Auxiliary Doors Closed

Appendix C Acoustic Baffle Test

In section 3.2.2, the measured BPF tone and Overall noise radiation patterns were described as the superposition of individual radiation patterns from the three separate noise outlets of the inlet (i.e., the inlet mouth, auxiliary doors, and fan exit). To better understand the acoustic properties of the supersonic inlets, it was important to investigate the individual noise contributions of the different noise paths. An acoustically treated baffle was constructed to allow the selective isolation and measurement of the inlet noise sources. The acoustic baffle, a 48 x 48 inch (122 x 122 cm) wooden panel faced on both sides with 1.5 inch (3.7 cm) acoustic foam, is shown in Figure 30. The effectiveness of the acoustic baffle (i.e., its ability to prevent noise transmission) was evaluated with the test procedure illustrated in Figure 30. A B & K microphone was placed 24 inches (61 cm) from the inlet at 0° to the inlet axis; the noise level at the microphone was then recorded with the baffle inserted between the inlet and microphone, and with the baffle removed. With the baffle in place, the average BPF tone level was lowered from 119dB to 90dB and the average overall noise was lowered from 126dB to 98dB. On a linear scale, the acoustic baffle prevented the transmission of approximately 96% of the acoustic power.

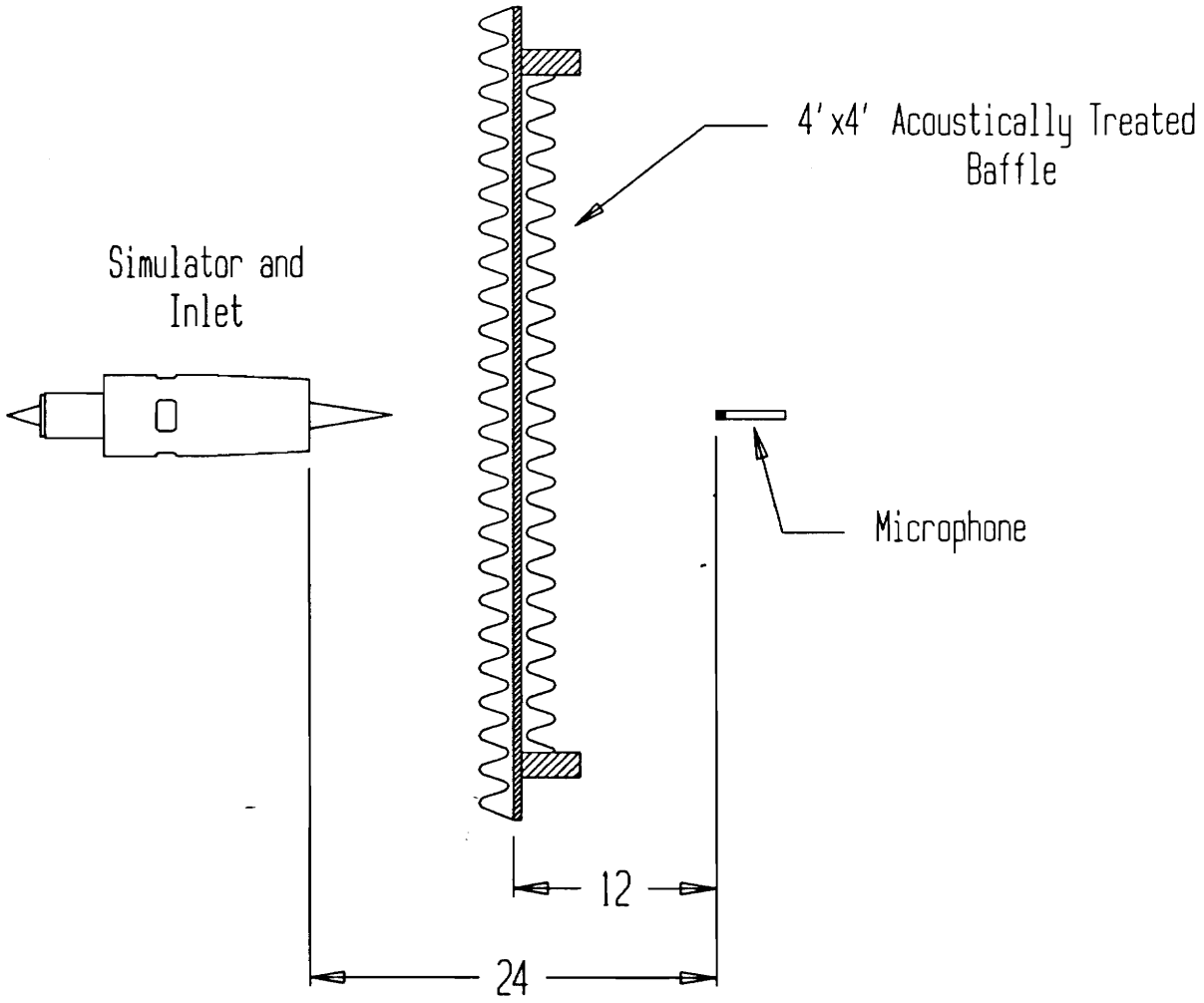

Figure 30. Set-up of Acoustic Baffle Effectiveness Test

The test configurations illustrated in Figure 31 were used to measure the noise radiation characteristics of the inlet mouth and auxiliary doors. Measurements of overall noise were made at four locations between 0° and 90° from the inlet centerline axis. The microphones were placed along a circular arc of 24 inch (61 cm) radius centered at the inlet cowl. With the baffle placed in test position one (as shown in Figure 31), only the noise radiated from the inlet mouth is allowed to reach the measurement field. In test position two, noise from both the inlet mouth and auxiliary doors can radiate to the microphone locations. In both test positions, the noise radiated from the fan exit is prevented from reaching the measurement field.

The acoustic baffle allows the observation of certain acoustic properties of the different noise outlets that cannot be measured when the radiation patterns are superimposed. Figure 32 illustrates the acoustic effect of choked flow in the throat of the Modified inlet. The narrowband spectra were recorded at the 0° microphone position with the acoustic baffle in test position one (allowing sound radiation from the inlet mouth only). As the simulator speed is increased from 75 PNC to 81 PNC, the level of the radiated noise is reduced abruptly. The large reduction in noise radiation is a result of sound attenuation caused by near-sonic throat flow at the higher fan speed.

The acoustic baffle also provides an indication of the radiation patterns of the different noise outlets of the test inlets. By treating the inlet mouth and auxiliary doors as uncorrelated sources (a reasonable approach with measurements of overall noise), it is possible to calculate the individual noise contribution of the auxiliary doors by:

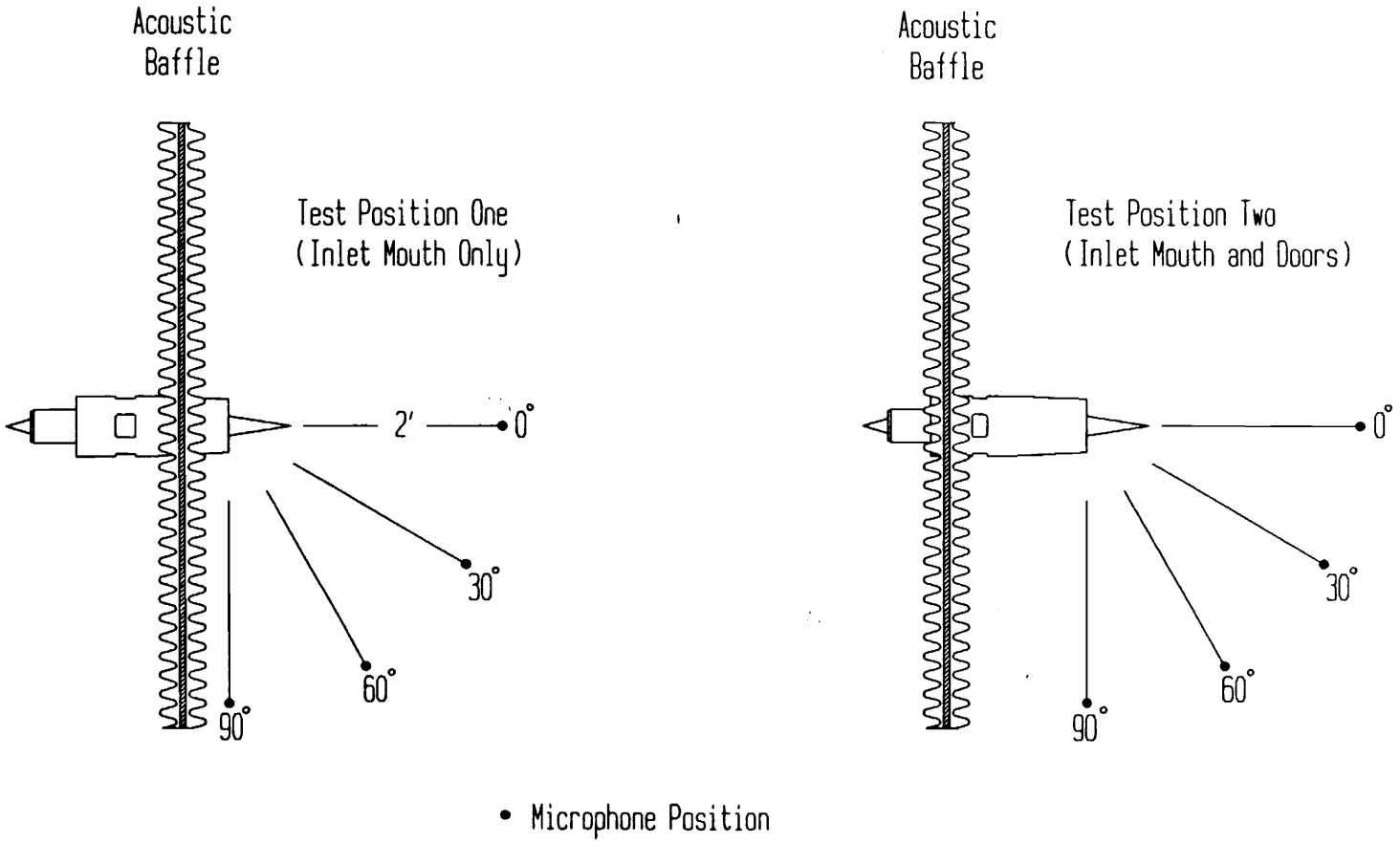

Figure 31. Acoustic Baffle Test Configurations and Microphone Locations

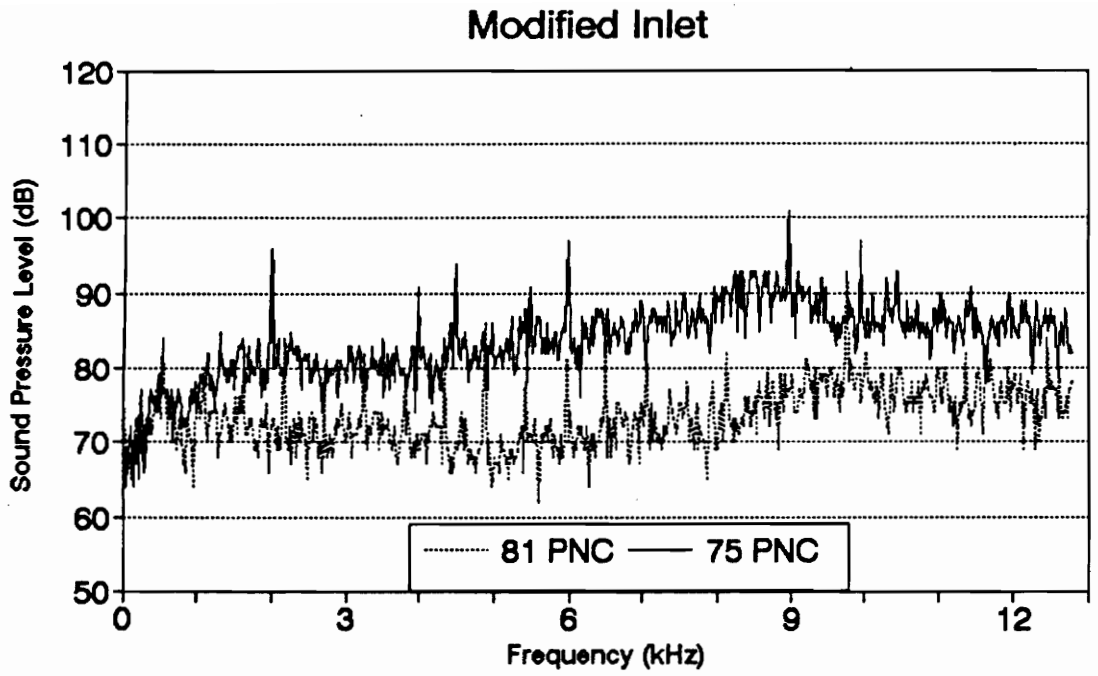

Figure 32. Effect of Choked Flow in the Inlet Throat

$$P_{doors} = P_{both} - P_{mouth} \quad (5)$$

In this equation, P_{doors} is the sound power radiated from the auxiliary doors, P_{mouth} is the measured sound power radiated from the inlet mouth, and P_{both} is the sound power of both sources as measured in test position two.

Figure 33 presents the noise radiation results of the acoustic baffle test. The values for the inlet mouth and "both" represent the measured quantities, while the values for the auxiliary doors are calculated from (5). For the Baseline inlet, the inlet mouth is seen to provide the predominant portion of the radiated noise from 0° to 60°. At 90°, however, the radiation of noise from the inlet mouth is reduced considerably, and the contribution of the auxiliary doors becomes predominant. This trend is consistent with the physical attributes of the Baseline inlet: a large door area radiating noise to the 90° microphone position. An important conclusion from these results is that the auxiliary doors provide a considerable portion of the radiated noise in the aft sector of the radiation field.

The Modified inlet provides a different distribution of the radiated noise. The mouth of the Modified inlet radiates less noise than that of the Baseline inlet because of the choked throat of the Modified inlet. For this reason, the auxiliary doors of the Modified inlet provide the predominant portion of the radiated noise from 30° to 90°. At 90°, the noise radiated from the auxiliary doors of the Modified inlet is 4dB lower than that radiated from the doors of the Baseline inlet; a reflection of the smaller area of the modified doors.

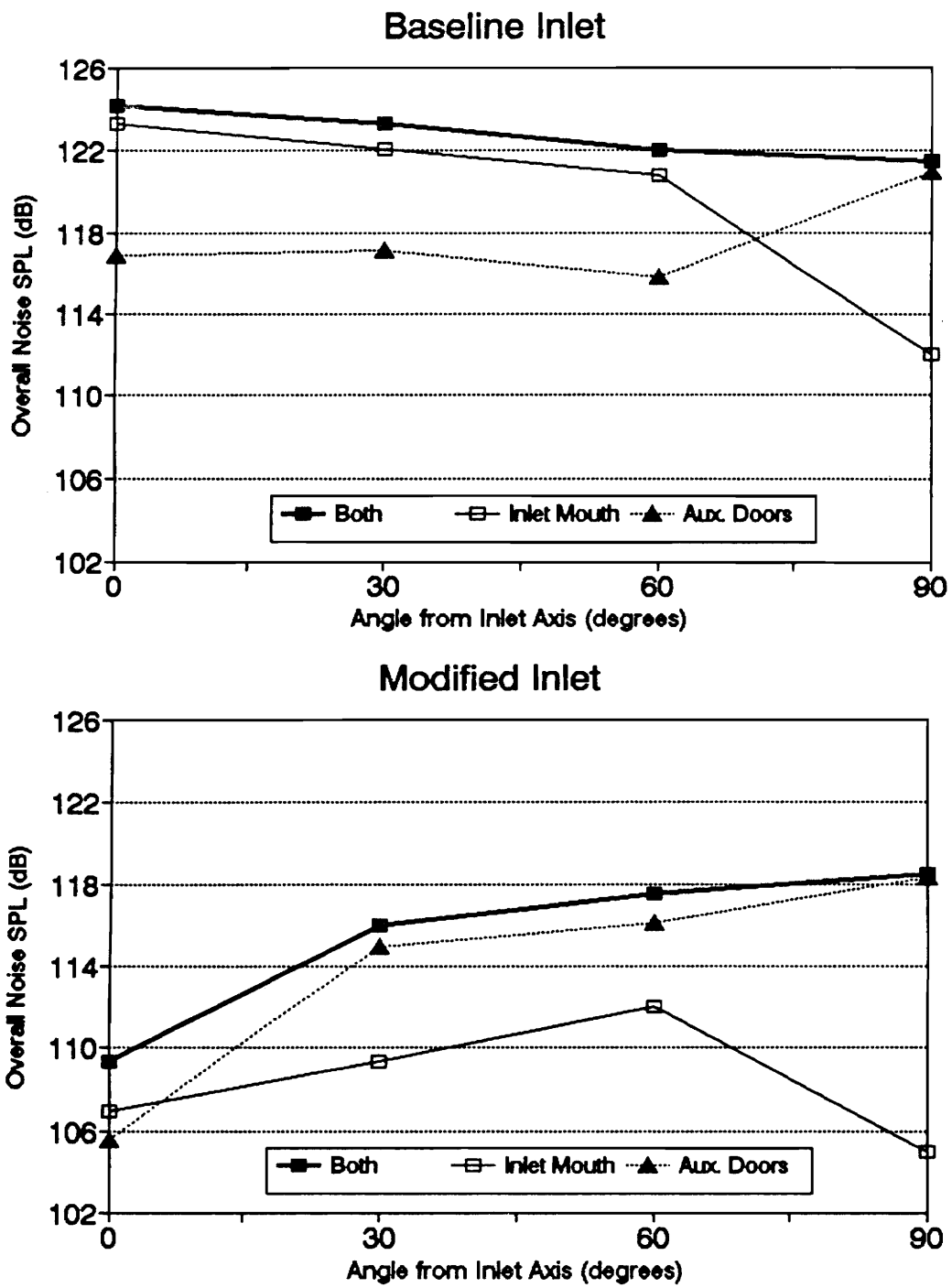

Figure 33. Radiation of Overall Noise from the Inlet Mouth and Auxiliary Doors, Baseline and Modified Inlets

References

1. Trefney, C.J., Wasserbauer, J.W., "Low-speed Performance of an Axisymmetric, Mixed-Compression, Supersonic Inlet With Auxiliary Inlets," NASA TP-2557, February 1986.

2. Woodward, R.P., Glaser, F.W., Lucas, J.G., "Low Flight Speed Acoustic Results for a Supersonic Inlet with Auxiliary Inlet Doors," NASA TM-83411, January 1983.

3. Koncsek, J. L., "Transonic and Supersonic Test for Improved Supersonic Inlet Performance," NASA CR 1977, March 1972.

4. Sorensen, N. E., Bencze, D. P., "Possibilities for Improved Supersonic Inlet Performance," AIAA Paper 73-1271, November 1973.

5. Smelter, D. B., Sorensen, N. E., "Analytic and Experimental Performance of Two Isentropic Mixed Compression Axisymmetric Inlets at Mach Numbers 0.8 to 2.65," NASA TN D-7320, June 1973.

6. Syberg, J., Turner, L., "Supersonic Test of a Mixed-Compresion Axisymmetric Inlet at angles of Incidence," NASA CR-165686, April 1981.

7. Wasserbauer, J. F., Cubbison, R. W., Trefney, C. J., "Low Speed Performance of a Supesonic Axisymmetric Mixed Compression Inlet with Auxiliary Inlets," AIAA Paper 83-1414, 1983.

8. Ball, W. H., Pickup, N., "Low Speed Performance and Acoustic Tests of an Axisymmetric Supersonic Inlet - Phase One Tests with Auxiliary Doors Closed," NASA CR-172390, October 1984.

9. Bangert, L. H., Burcham, F. W., Mackall, K. G., "YF-12 Inlet Suppression of Compressor Noise: First Results," AIAA Paper 80-0099, January 1980.

10. Bangert, L. H., Feltz, E. P., Godby, L. A., Miler, L. D., "Aerodynamic and Acoustic Behavior of a YF-12 Inlet at Static Conditions," NASA CR-163106, January 1981.

11. Topol, D. A., Holhubner, S. C., Mathews, D. C., "A Reflection Mechanism for Aft Tone Fan Noise from Turbofan Engines," AIAA Paper 87-2699, October 1987.

12. Topol, D. A., "Rotor Wake/Stator Interaction Noise-Predictions Versus Data," AIAA Paper 90-3951, October 1990.

13. Tyler, J. M., Sofrin, T.G., "Axial Compressor Noise Studies," SAE Transactions, Vol. 70, 1962.

14. Homicz, G. F., Lordi, J. A., "A Note on the Radiative Directivity Patterns of Duct Acoustic Modes," Journal of Sound and Vibration, December 1975.

15. Feiler, C. E., and Groenweg, J. F., "Sumary of Forward Velocity Effects on Fan Noise," AIAA Paper 77-1319, October 1977.

16. Oates, G. C., "Aerothermodynamics of Aircraft Engine Components," American Institute of Aeronautics and Astronautics, 1st edition, 1985, pp. 477-584.

17. Nuckolls, W. E., Ng, W. F., "Fan Noise Reduction from a Supersonic Inlet during Simulated Aircraft Approach," to be presented in ASME IGTI Conference, Cincinnati, OH, May 1993.

Vita

Kevin Detwiler was born in Cumberland, Maryland on September 2, 1969. He and his family then lived in North Carolina, Brazil, and Canada before settling in Windham, Maine where he entered elementary school. Growing up on the Presumpscott River, the author developed his interest in fishing, hiking, and outdoor life. After graduating from Windham High School in June 1987, he began his undergraduate studies in mechanical engineering at the University of Maine at Orono. During the summer months, he worked at S & D Manufacturing, his father's tire retreading shop in Gorham, Maine. In May 1991, he graduated with a Bachelor of Science degree in mechanical engineering. The following fall, he started his graduate studies at Virginia Tech while working as a graduate teaching assistant for the Mechanical Engineering Department. In the spring, he became a graduate assistant for Dr. Wing Ng and began the research for this thesis. The author defended this work on April 12, 1993, and plans to enter the diploma course at the von Karman Institute for Fluid Dynamics in the fall.

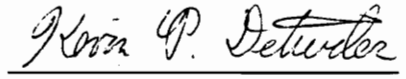

Kevin P. Detwiler